PETROLEUM RECOVERY INSTITUTE

THE APPLICATION OF CONTINUOUS THERMODYNAMICS TO HEAVY OIL RECOVERY PROCESSES

FINAL REPORT SUBMITTED TO CANMET

UNDER CONTRACT NO. 23440-8-9225/01-SQ

MARCH 31, 1990

BY

S. L. KOKAL AND S. G. SAYEGH

91-02598/

THE APPLICATION OF CONTINUOUS THERMODYNAMICS TO HEAVY OIL RECOVERY PROCESSES

Final Report submitted to CANMET
under Contract No. 23440-8-9225/01-SQ

March 31, 1990

by

S. L. Kokal and S. G. Sayegh

91 pp

MICROMEDIA

TABLE OF CONTENTS

List of Tables	iii
List of Figures	iv
Acknowledgements	vi
Abstract	vii
CHAPTER 1 - INTRODUCTION	1
CHAPTER 2 - PHASE EQUILIBRIA CALCULATIONS	3
2.1 Discrete Component Mixtures	3
2.2 Semi-Continuous Mixtures	7
2.3 Gaussian Quadrature Treatment of Semi-Continuous Mixtures	11
CHAPTER 3 - CONTINUOUS THERMODYNAMIC METHODOLOGY	14
3.1 Distribution Functions	14
3.2 Quadrature Methods	15
3.3 Distribution Data	18
3.4 Specific Gravity	19
3.5 Critical Properties of quadrature Pseudo-Components	20
3.6 Volumetric Calculations	21
3.7 Implementation of Semi-Continuous Thermodynamic Approach	22
CHAPTER 4 - RESULTS AND DISCUSSION	25
4.1 N-Paraffins	25
4.2 Gas-Condensate System	26
4.3 Light Oil Systems	27
4.3.1 Canadian Light Oil	27
4.3.2 U.S. Light Oil	29
4.4 Heavy Oil Systems	29
4.4.1 Lindbergh Heavy Oil	30
4.4.2 Lone Rock Heavy Oil	34
CHAPTER 5 - CONCLUSIONS	36

REFERENCES 38

TABLES 47

FIGURES 54

LIST OF TABLES

Table 1	Sensitivity results for 24 components n-paraffin example at 500 kPa
Table 2	Hoffman et al.[70] reservoir gas composition
Table 3	Binary interaction coefficients used in this study
Table 4	Dew point results for a reservoir gas mixture of Hoffman et al.[70] at 93.8°C
Table 5	Gas-oil ratios for a reservoir gas mixture of Hoffman et al.[70] at 93.9°C
Table 6	Comparison of liquid mixture densities for flashed reservoir gas mixture of Hoffman et al.[70] at 93.9°C
Table 7	Properties of oil # 2 and hydrocarbon solvent of Wu and Fish[72]
Table 8	Comparison of saturation pressures for oil # 2 of Wu and Fish[72] at 62°C
Table 9	Comparison of saturated liquid densities for oil # 2 of Wu and Fish[72] at 62°C
Table 10	Comparison of saturated liquid densities for oil # 2 of Wu and Fish[72] at 62°C
Table 11	Properties of Maljamar separator oil
Table 12	Properties of Lindbergh heavy oil and its fractions
Table 13	Properties of Lone Rock heavy oil and its fractions

LIST OF FIGURES

Figure 1 Finite-component and infinite-component mixtures

Figure 2 The Γ density distribution function. Effect of distribution parameters

Figure 3 Gas-chromatograph simulated distillation curves for typical petroleum fluids

Figure 4 Typical molar distributions using gas-chromatograph simulated distillation

Figure 5 Density curves as a function of carbon number and aromaticity

Figure 6 Flow chart for calculating the densities of quadrature pseudo-components

Figure 7 Feed composition of the 24 components n-paraffin mixtures

Figure 8 Gas-oil ratios for a natural gas mixture at 93.9°C

Figure 9 Comparison of density predictions for gas-condensate of Hoffman et al.[70]

Figure 10 Saturation pressures for oil 2 with HC solvent data of Wu and Fish[72]

Figure 11 Comparison of density of oil 2

Figure 12 Phase behavior of mixtures of CO_2 with Maljamar separator oil at 32.2°C

Figure 13 Molar distribution of Lindbergh heavy oil and its fractions

Figure 14 Phase behavior of Lindbergh heavy oil/CO_2 mixtures

Figure 15 Phase behavior of Lindbergh de-asphalted oil/CO_2 mixtures

Figure 16 Phase behavior of Lindbergh Fraction 2/CO_2 mixtures

Figure 17 Phase behavior of Lindbergh Fraction 1/CO_2 mixtures

Figure 18 Density of Lindbergh heavy oil/CO_2 mixtures

Figure 19 Density of Lindbergh de-asphalted oil/CO_2 mixtures

Figure 20 Density of Lindbergh Fraction 2/CO_2 mixtures

Figure 21 Density of Lindbergh Fraction 1/CO_2 mixtures

Figure 22 Molar distribution of Lone Rock heavy oil and its fractions

Figure 23 Phase behavior of Lone Rock heavy oil/CO_2 mixtures

Figure 24 Phase behavior of Lone Rock de-asphalted oil/CO_2 mixtures

Figure 25 Phase behavior of Lone Rock Fraction 2/CO_2 mixtures

Figure 26 Phase behavior of Lone Rock Fraction 1/CO_2 mixtures
Figure 27 Density of Lone Rock heavy oil/CO_2 mixtures
Figure 28 Density of Lone Rock de-asphalted oil/CO_2 mixtures
Figure 29 Density of Lone Rock Fraction 2/CO_2 mixtures
Figure 30 Density of Lone Rock Fraction 1/CO_2 mixtures

ACKNOWLEDGEMENTS

Figure 1: Copyright by American Chemical Society, reprinted by permission.

The authors would like to thank Mr. Douglas Fisher for use of his program "INSIGHT" for least squares regression of the distribution functions. Financial support from Energy Mines and Resources (Canada) is acknowledged. Thanks are also due to Dr. A.E. George of Energy Mines and Resources for fruitful discussion.

ABSTRACT

The injection of light hydrocarbon gases or carbon dioxide into crude oil reservoirs is a viable enhanced oil recovery (EOR) method. The design of such EOR scheme requires a reliable predictive method for calculating the phase behavior and physical properties of solvent/crude oil mixtures. This study deals with the application of principles of continuous thermodynamics to light and heavy oil systems using the Peng-Robinson (PR) equation of state (EOS). The composition of the high molecular weight components in a reservoir oil is described by a continuous distribution function of some characterizing quantity eg. molecular weight or the boiling temperature. Numerical Gaussian quadrature methods were used to generate pseudo-components and their mole fractions from distribution data. Several examples are presented for phase equilibria of solvent/crude oil systems.

The results showed that semi-infinite distribution functions, such as Γ function, cannot be applied to all cases, eg. dew point calculations. Gauss-Legendre quadrature method coupled with spline fitting worked best for heavy oil systems. Semi-continuous descriptions were also successful in correlating the densities of oil/gas mixtures using the volume translated Peng-Robinson equation of state.

CHAPTER 1

INTRODUCTION

The term continuous mixtures has been coined to deal with mixtures that have very many components belonging to homologous series. Examples of such mixtures include crude oils, the heavy ends of natural gas liquids, and some polymer solutions. The extremely large number of components in such mixtures makes it prohibitively cumbersome to try and account for each and every one of them. For example, to measure the mole fractions of all of these components in a solution is difficult. A more practical approach would be to measure the frequency distribution of the range of molecular weights as shown in Figure 1. In a system with a limited number of components the frequency distribution is in the form of a histogram with one column per component. In mixtures with many components the columns blend together to give a continuous curve. Of course the two types of distributions could coexist in which case the mixture is referred to as semi-continuous. An example of a semi-continuous mixture is a crude oil in which is dissolved carbon dioxide and nitrogen.

What follows is a summary of works in the literature dealing with the various aspects of continuous thermodynamics. This will be followed with a more detailed discussion of some of the works that are particularly relevant to the present study in the section on phase equilibria calculations.

The general framework of continuous thermodynamics has been studied by several authors[1-5]. This framework has been applied to a number of processes such as isothermal flash calculations[4,6-9], adiabatic flash

calculations[10], enthalpy calculations[11], distillation computations[4,12], and liquid-liquid equilibria[7,13]. The phase behavior calculations have been carried out using a variety of equations of state such as the Peng-Robinson[8,14-17], Soave-Redlich-Kwong[6,7,11,18,19], UNIFAC[20,21], perturbed hard chain[22], and other statistical thermodynamical models[1,23].

Within the framework of continuous thermodynamics it is necessary to use some method to describe the property distributions. Examples of this include Gaussian quadrature[6,10,24], spline fitting[18], orthogonal polynomials[19,25], and variational methods[26]. Most of the authors use a univariate description of the continuous fractions, in other words they describe that fraction by the frequency distribution of one property such as the molecular weight or the normal boiling point. This may not be adequate for certain mixtures, such as those containing members of different homologous series, in which case multivariate distributions should be used[7,27].

Fossil fuels provide an ideal framework for the application of continuous thermodynamics, consequently there are a large number of such works on petroleum liquids[13-17,20,27-36] natural gases[6,7,34,37,38], and petroleum solids such as waxes[39] and asphaltenes[40]. Biochemical systems could also exist in a polydispersed state to which the methods of continuous thermodynamics could be applied, and this has been demonstrated for mixtures of fatty alcohols[24].

CHAPTER 2
PHASE EQUILIBRIA CALCULATIONS

Phase equilibrium calculations may be performed using a cubic equation of state which describes both the vapor and liquid properties. The general criterion for the equilibrium of phases at a given pressure and/or temperature is the equality of chemical potential for every component in the mixture in all phases. We give an example for a flash calculation below; however the procedure can be modified easily for other types of phase behavior calculations.

A flash calculation is a general algorithm for determining the amount and composition of the phases that a mixture will split into when allowed to reached equilibrium at a specified temperature and pressure. The commonly used procedure for discrete component mixtures will first be summarized followed by the method for continuous or semi-continuous mixtures.

2.1 Discrete Component Mixtures:

Assume one mole of a feed stream of known composition is to be flashed at a constant temperature T and pressure P to produce ξ moles of vapor and λ moles of liquid at equilibrium. An overall mass balance gives:

$$\xi + \lambda = 1 \tag{2.1}$$

In general, the feed may be any number of moles in which case ξ and λ can be thought of as the fractions of the feed that are in the liquid and vapor phase, respectively. A component mass balance for every component i

in the mixture yields the following set of equations:

$$z_i = (1 - \xi)x_i + \xi y_i \qquad i = 1, 2, \ldots, n \qquad (2.2)$$

where:

n = number of components in the mixtures

x_i = mole fraction of component i in the liquid phase

y_i = mole fraction of component i in the vapor phase

By definition, the mole fractions in any phase have to be normalised which leads to the following two equations:

$$\sum_i x_i = 1 \qquad (2.3)$$

$$\sum_i y_i = 1 \qquad (2.4)$$

Finally, thermodynamic equilibrium requires that the fugacity (or chemical potential) of each component in the liquid phase be the same as the fugacity of that component in the vapor phase. This leads to the following set of equilibrium equations:

$$f_i^L = f_i^V \qquad i = 1, 2, \ldots, n \qquad (2.5)$$

By definition, the fugacity coefficient of component i in the liquid phase, ϕ_i^L, is related to its fugacity by the equation:

$$f_i^L = x_i \phi_i^L P \qquad (2.6)$$

And the same relationship applies to the vapor phase, giving:

$$f_i^V = x_i \phi_i^V P \qquad (2.7)$$

Combining equations 2.5 - 2.7:

$$y_i \phi_i^V = x_i \phi_i^L \qquad i = 1, 2, \ldots, n \qquad (2.8)$$

where:

ϕ_i^V and ϕ_i^L = the fugacity coefficients of component i in the vapor and liquid phases, respectively.

Fugacity coefficients are generally calculated from equations of state or other correlations. The Peng-Robinson[41] equation of state is selected for this work which leads to the following derivation of the expression for the fugacity coefficients:

The basic equation of state is written as:

$$P = \frac{RT}{v - b} - \frac{a(T)}{v(v+b) + b(v-b)} \qquad (2.9)$$

Where:

$$b = \sum_i x_i b_i \qquad (2.10)$$

$$b_i = \sum 0.07780 \frac{RT_{ci}}{P_{ci}} \qquad (2.11)$$

$$a = \sum_i \sum_j x_i x_j a_{ij} \qquad (2.12)$$

$$a_{ij} = (1 - \delta_{ij}) a_i^{1/2} a_j^{1/2} \qquad (2.13)$$

$$a_i = \left\{ 0.45724 \frac{R^2 T_{ci}^2}{P_{ci}} \right\} \left\{ 1 + (0.37464 + 1.54266\, \omega_i - 0.26992\, \omega_i^2) \left(1 - \left[\frac{T}{T_{ci}} \right]^{1/2} \right) \right\}^2 \qquad (2.14)$$

P = pressure

R = gas constant

T = absolute temperature

v = molar volume

T_{ci} = critical temperature of component i

P_{ci} = critical pressure of component i

ω_i = acentric factor of component i

Equation 2.9 may be rewritten in terms of the compressibility factor, Z, as:

$$Z^3 + (1 - B)Z^2 + (A - 3B^2 - 2B)Z - (AB - B^2 - B^3) = 0 \qquad (2.15)$$

where:

$$Z = \frac{Pv}{RT} \qquad (2.16)$$

The Peng-Robinson equation always gives the same value for the compressibility factor at the critical point, Z_c:

$$Z_c = 0.307 \qquad (2.17)$$

Standard thermodynamics gives the relationship between the fugacity of component k, f_k, and pressure as:

$$ln\ \phi_i = \frac{1}{RT}\int_0^P \left(\frac{v_i}{RT} - \frac{1}{P} \right) dP \qquad (2.18)$$

or more conveniently for pressure-explicit equations of state:

$$ln\ \phi_i = \int_v^\infty \left(\frac{\partial P}{\partial n_i} - \frac{RT}{V} \right) dV - RT\ ln\ z \qquad (2.19)$$

Substituting from equations 2.6 to 2.13 into 2.15 and performing the integration:

$$\ln \phi_k = \frac{b_k}{b} (Z - 1) - \ln (Z - b) - \frac{A}{2\sqrt{2}\, B}$$

$$\left(\frac{2 \sum_i x_i a_{ik}}{a} - \frac{b_k}{b} \right) \ln\left(\frac{Z + 2.414\, B}{Z - 0.414\, B} \right) \qquad (2.20)$$

The above equations constitute the set required to solve for the values of y_i, x_i and ξ.

2.2 Semi-Continuous Mixtures:

As was mentioned in the introduction and depicted schematically in Figure 1, continuous mixtures are characterized by their distribution function, F(I), of a characteristic property, I. Semi-continuous mixtures contain both discrete components as well as continuous ones, and hence represent the more common case in petroleum mixtures. The thermodynamic analysis of such mixtures will now be summarized as presented by Cotterman et al.[6,7].

The distribution function is normalized to yield the following relationship:

$$\int_{I_{min}}^{I_{max}} F(I)\, dI = 1 \qquad (2.21)$$

where I_{min} and I_{max} are the minimum and maximum values of I for the mixtures under study.

In analogy to equation 2.3 and 2.4, one may now write the mole

fraction normalization equations for the semi-continuous feed, liquid, and vapor phases, respectively, as:

$$\sum_1 z_i + \eta^F \int F^F(I)\, dI = 1 \qquad (2.22)$$

$$\sum_1 x_i + \eta^L \int F^L(I)\, dI = 1 \qquad (2.23)$$

$$\sum_1 y_i + \eta^V \int F^V(F)\, dI = 1 \qquad (2.24)$$

where

$i = 1,2,\ldots,n$

n = number of *discrete* components in the mixture

η^F, η^L, and η^V = mole fractions of continuous component in the feed, liquid, and vapor phases, respectively

F^F, F^L, and F^V = distribution functions of continuous component in the feed, liquid, and vapor phases, respectively.

The component mass balance equations may now be written, in analogy to equation 2.2, for the discreet components as:

$$z_i = \xi\, y_i + (1 - \xi)x_i \qquad i = 1,2,\ldots,n \qquad (2.25)$$

and for the continuous fraction as:

$$\eta^F F^F(I) = \xi\eta^V F^V(I) + (1 - \xi)\eta^L F^L(I) \qquad (2.26)$$

Since the vapor and liquid phases are in equilibrium, then the fugacities of each component in both phases are equal, which leads to the following condition for the discrete components:

$$f_i^V = f_i^L \qquad i = 1, 2, \ldots, n \qquad (2.27)$$

as previously presented in equation 2.5. And for the continuous fraction:

$$f^V(I) = f^L(I) \qquad \text{for all values of } I \qquad (2.28)$$

Equation 2.28 is a result of the functional analysis of the equilibrium conditions as presented by Salacuse and Stell[23] and later by Kehlen et al.[4]. Equations 2.27 and 2.28 may be reformulated in terms of the fugacity coefficients, in analogy to equation 2.8, as:

$$y_i \phi_i^V = x_i \phi_i^L \qquad i = 1, 2, \ldots\ldots, n \qquad (2.29)$$

for the discrete components, and:

$$\eta^V F^V(I) \phi^V(I) = \eta^L F^L(I) \phi^L(I) \qquad \text{for all values of } I \qquad (2.30)$$

for the continuous fraction.

Kehlen, Ratzsch, and co-workers[4,5,12,13,20,30,42,43] presented extensive analyses of continuous thermodynamics, and applied their methods to a variety of problems such as flash and distillation calculations. They formulated the conditions of equilibrium (c.f. equations 2.5 and 2.8) in terms of the chemical potentials in the vapor and liquid phases, μ^V and μ^L, as:

$$\mu^L(I) = \mu^V(I) \qquad \text{for all values of } I \qquad (2.31)$$

Equation 2.31 is analogous to 2.28 or 2.30. They maintained the general form of the integrals of the characteristic distribution function throughout their analyses, which has the advantage of internal consistency and an analysis well suited for continuous mixtures. On the other hand, the application of their method requires that the equation of state selected

for the calculations be rederived in continuous form for the specific distribution function selected.

Du and Mansoori[8,15,16] derived algorithms for the continuous thermodynamics of mixtures based on the minimization of the Gibbs free energy. They used an equilibrium condition analogous to equation 2.11, and, in addition, assumed that the first three derivatives of the chemical potential with respect to the distribution parameter exist. From this assumption they obtained the following equations:

$$\frac{\partial^n \mu^L}{\partial I^n} = \frac{\partial^n \mu^V}{\partial I^n} \qquad n = 1,\ 2,\ \text{and}\ 3 \tag{2.32}$$

Du and Mansoori[8,15,16] applied their method to the van der Waals and the Peng-Robinson (c.f. equations 2.9) equations of state. The a and b parameters were correlated as cubic functions of molecular weight so that equation 2.32 may be applied, though other forms may be used. As with the method of Kehlen, Ratzsch, and co-workers discussed above, the algorithm of Du and Mansoori requires that the equation of state be rederived for each form of the distribution function.

Willman and Teja[37,38] derived a semi-continuous thermodynamic formulation of the phase behavior of natural gas and petroleum mixtures in terms of fugacity coefficients for the vapor phase and activity coefficients for the liquid phase. This has the advantage that different equations of state may be used for each of these phases. For example, in their second paper[62] they used the virial equation for the vapor phase and the regular solution theory for the liquid. By characterizing the

parameters of their equations of state in terms of effective carbon numbers they were able to satisfactorily predict the dew points of a number of natural gas mixtures.

Cotterman *et al.*[6,7,29,32,33] approximated the integrals of the distribution functions with summations obtained from Gaussian quadrature, and were able to derive a framework that is applicable to both continuous and semi-continuous mixtures. This is a big advantage since semi-continuous mixtures commonly occur in the petroleum industry. Furthermore, existing phase equilibrium programs can be very easily modified to accommodate this method since the numerical quadrature is applied before the phase equilibria calculations are carried out. Furthermore, the procedure, as presented before, is general enough that any equation of state may be used, provided that the same equation is used for both the vapor and liquid phases. In addition, any form of the distribution function may be used such as spline fits[18], exponential decays[14], gamma functions[6] or orthogonal polynomials. Accordingly, the Cotterman *et al.*[6] procedure was adopted for the present work.

2.3. Gaussian Quadrature Treatment of Semicontinuous Mixtures:

As mentioned in the introduction, the continuous distribution functions may be handled in a variety of ways such as spline fitting or orthogonal polynomials. In this treatment we will concentrate on the method of Gaussian quadrature as applied by Cotterman and Prausnitz[6]. For more details on Gaussian quadrature the reader is referred to Stroud and Secrest[44]. In this method the integration of the continuous distribution curve is replaced by a finite sum of the value of the distribution function

at specified quadrature points multiplied by a weighting function.

$$\int F(I)\, dI = \sum_{j=1}^{m} w_j F(I_j) \qquad (2.33)$$

where:

w_j = the weighting factor for the j^{th} quadrature point

I_j = the value of the characteristic property at the j^{th} quadrature point

m = the number of quadrature points or the order of the approximation

Substituting equation 2.33 into equations 2.22 to 2.24, the mole fraction normalization equations become:

$$\sum_{1} z_i + \eta^F \sum_{j=1}^{m} w_j F^F(I_j) = 1 \qquad (2.34)$$

$$\sum_{1} x_i + \eta^L \sum_{j=1}^{m} w_j F^L(I_j) = 1 \qquad (2.35)$$

$$\sum_{1} y_i + \eta^V \sum_{j=1}^{m} w_j F^V(I_j) = 1 \qquad (2.36)$$

The discrete component mass balance equation (equation 2.25) remains valid and is rewritten in equation 2.37:

$$z_i = \xi\, y_i + (1 - \xi)x_i \qquad i = 1, 2, \ldots, n \qquad (2.37)$$

While for the continuous fraction equation 2.26 becomes:

$$\eta^F F^F(I_j) = \xi\eta^V F^V(I_j) + (1 - \xi)\eta^L F^L(I_j) \qquad j = 1, 2, \ldots, m \qquad (2.38)$$

The equilibrium conditions in terms of fugacity coefficients, equations 2.29 and 2.30, become:

$$y_i \phi_i^V = x_i \phi_i^L \qquad i = 1, 2, \ldots, n \tag{2.39}$$

for the discrete components, and:

$$\eta^V F^V(I_j) \phi^V(I_j) = \eta^L F^L(I_j) \phi^L(I_j) \qquad j = 1, 2, \ldots, m \tag{2.40}$$

for the continuous fractions. Note that the values of w_j do not appear in equations 2.38 and 2.40 since they cancel out from both sides. The fugacity coefficients can be calculated from equations 2.9 to 2.20 directly for the discrete components, and by substituting the product $\eta w F$ for the mole fractions for the continuous fraction as shown below:

$$z_j = \eta^F w_j F^F(I_j) \qquad j = 1, 2, \ldots, m \tag{2.41}$$

$$x_j = \eta^L w_j F^L(I_j) \qquad j = 1, 2, \ldots, m \tag{2.42}$$

$$y_j = \eta^V w_j F^V(I_j) \qquad j = 1, 2, \ldots, m \tag{2.43}$$

CHAPTER 3

CONTINUOUS THERMODYNAMIC METHODOLOGY

3.1 Distribution Functions:

The continuous fraction is generally described by an analytical distribution function. The continuous distribution variable could be the normal boiling point, T_b, or the molecular weight, or the effective carbon number, etc. As mentioned earlier, the continuous distribution functions may be handled in a variety of ways such as spline fitting, or orthogonal polynomials. A three-parameter gamma-distribution function was used by Whitson[45] and later by Cotterman and Prausnitz[6] to describe the C_{7+} fraction. These parameters are generally fitted to the experimental molar and weight distributions data. It has been shown by Whitson[45], and many others[14,15,17,46,47] that petroleum fluids exhibit an exponential distribution with the molecular weight or carbon number. An experimental decay distribution function is of the form:

$$F(I) = A \exp (- B I) \tag{3.1}$$

where A and B are the distribution parameters. Another distribution function which is commonly used for petroleum fluids is the gamma (Γ) distribution function given by:

$$F(I) = \frac{(I - I_{min})^{\alpha-1}}{\beta^{\alpha}\,\Gamma(\alpha)} \exp\left[\left(- \frac{I - I_{min}}{\beta}\right)\right] \tag{3.2}$$

where α, β, I_{min} are the distribution parameters and Γ is the gamma function. Figure 2 shows the relative effect of the three parameters on the distribution. When $\alpha = 1$, this reduces to the exponential distribution function 3.1. Some of the properties of the gamma distribution function

are:

$$F(\infty) = 0$$

$$\text{mean:} \quad \theta = \alpha\beta + I_{min}$$

$$\text{variance:} \quad \sigma^2 = \alpha\beta^2$$

$$\int_{I_{min}}^{\infty} F(I)\, dI = 1$$

The gamma distribution function is an example of semi-infinite distribution. A more realistic distribution for petroleum fluids is the truncated gamma distribution since carbon numbers greater than 100 are generally not encountered in such fluids. A truncated distribution was proposed by Behrens and Sandler[14] and Shibata et al.[46] A truncated exponential distribution is given by:

$$F(I) = A\, e^{-BI} \qquad I_{min} \le I \le I_{max} \le \infty \tag{3.3}$$

The parameters of the truncated distribution are B, I_{min} and I_{max}. "A" is set by normalization. Other types of distribution functions have also been used. Peng[17] used the beta distribution function, Willman and Teja[27] used a bivariate log normal distribution function to represent the molar composition vs. specific gravity and normal boiling point of the mixture. A description of the distribution functions can be found in a probability and statistical book[48].

3.2 Quadrature Methods:

Quadrature methods are schemes of integrating continuous analytical functions where the integrals are replaced by a finite sum of the value of the function at specified quadrature multiplied by a weighting function

$$\int F(I)\, dI = \sum_{j=1}^{n} w_j\, F(q_j) \tag{3.4}$$

where w_j is the weighting factor for the jth quadrature point, q_j is the value of the characteristic property at the jth quadrature point and m is the number of quadrature points. The gamma distribution functions can be approximately integrated using the generalized-Gauss-Laguerre quadrature methods[49]. The m-point quadrature formula is

$$\int_0^{\infty} F(u)\, du = \sum_{j=1}^{m} w_j\, u_j^{1-\alpha}\, e^{-u_j}\, F(u_j) \tag{3.5}$$

where w_j and u_j are the weighting factors and quadrature points respectively. The quadrature points are the zeros of the generalized Laguerre polynomials and the weighting factors are given by

$$w_j = \frac{n!\ \Gamma(n+\alpha)\ u_j}{\left(L_{n+1}^{\alpha-1}\ (u_j) \right)^2} \tag{3.6}$$

Substituting equation 3.2 into equation 3.5 and after some transformation, the quadrature points are given by

$$I_i = u_i \beta + I_{min} \tag{3.7}$$

The effective mole fraction of the distribution F(I) are given by

$$q_j = \frac{\eta\ w_j}{\Gamma(\alpha)} \tag{3.8}$$

where η is the mole fraction of the continuous fraction.

When analytical distribution functions do not fit the distribution data, one can use simple cubic splines[18] and use a simple Gauss-Legendre

quadrature method for generating the quadrature pseudo-components. This method, however, is not very accurate for values of small n. The Legendre polynomial roots listed in the literature are usually for integration limits of a variable, τ, that go from -1 to +1. These are scaled to practical limits of I using the transformation:

$$I = \left\{ \frac{\tau\,(I_{max} - I_{min}) + I_{max} + I_{min}}{2} \right\} \qquad (3.9)$$

Accordingly, the general integral of equation (3.4) is written in terms of τ as

$$\int_{I_{min}}^{I_{max}} F(I)\, dI = \frac{I_{max} - I_{min}}{2} \int_{-1}^{+1} F\left(\frac{\left(I_{max} - I_{min} \right) \tau + I_{max} + I_{min}}{2} \right) d\tau \qquad \ldots.(3.10)$$

Combining equation (3.4) with equations (3.9) and (3.10) gives:

$$\int_{I_{min}}^{I_{max}} F(I)\, dI = \frac{I_{max} - I_{min}}{2} \sum_{i=}^{n} w_i F\left(\frac{\left(I_{max} - I_{min} \right) \tau_i + I_{max} + I_{min}}{2} \right) d\tau \qquad \ldots.(3.11)$$

The quadrature points are given by:

$$I_i = \left(\frac{\left(I_{max} - I_{min} \right) \tau_{Li} + I_{max} + I_{min}}{2} \right) \qquad i = 1,..n \qquad (3.12)$$

and the effective mole fractions are given by:

$$w_i = \frac{I_{max} - I_{min}}{2} w_{Li} \qquad i = 1,..n \qquad (3.13)$$

The roots of the Legendre polynomials, τ_{Li}, and their associated weighting factors, w_{Li}, can be obtained from a standard mathematical handbook.

The procedure essentially becomes the generation of discrete pseudo-components at the quadrature points with the mole fractions determined by the weighting of the quadrature points. The quadrature pseudo-components are then used to represent the continuous fraction in subsequent equilibrium calculations. One great advantage of this method is that existing discrete EOS programs can be used without modifications by assigning the pseudo-components at the correct quadrature points. This method also eliminates the arbitrariness from the general "trial and error" methods which are used for the selection of pseudo-components.

3.3 Distribution Data:

The first step in the implementation of the semi-continuous thermodynamic analysis is the determination of distribution function parameters for the continuous fractions. The C_{7+} fraction or the "heavies" are generally characterized by their molecular weight, specific gravity and/or the boiling point. In some cases distillation of the C_{7+} fraction is performed to obtain boiling points, specific gravities, molecular weights and molar distribution of the distillation "cuts". This method, however, is expensive and time consuming and the data are not generally available.

Rapid advancements in chromatographic techniques has lead to the development of simulated distillation on the gas chromatograph. The results from these methods yield boiling temperatures and weight fraction as a function of the equivalent molecular weights. These data can be manipulated to yield molar distributions. Typical simulated distillation results using the gas chromatograph for a gas condensate, a light and a heavy oil are

shown in Figures 3 and 4. Specific gravity data is generally not obtained with this technique. Another disadvantage with this method is that only partial analysis, up to C_{40}, can be obtained. However, capillary columns used in conjunction with high temperature simulated distillation gas chromatographs can go to higher (C_{70}) molecular weights.

Another technique to obtain molar distributions of petroleum fluids is the use of gel permeation chromatography (GPC). It was used by Leontaritis[50] and is routinely used for molecular weight distributions[51,52] of very heavy components eg. asphaltenes. Results from GPC must be interpreted with caution since the molecular weight calibration of the GPC columns is based on polystyrene standards which are very different from those of petroleum fluids. Also the GPC technique is applicable to the higher molecular weight samples.

Whenever molar distributions of the C_{7+} fraction is available, it can be fitted to some kind of distribution function to obtain distribution parameters. When the molar distributions are not available, a simple approximate technique can be used to obtain the distribution parameters as described below. As mentioned earlier and also demonstrated by others, petroleum fluids can be adequately described by gamma or simply the exponential decay distribution functions.

3.4 Specific Gravity:

Specific gravity distribution is normally not available for the C_{7+} fraction. A generalized specific gravity function was reported by Yarborough[53] where the results of specific gravity measurements on narrow

boiling fractions obtained from several true boiling point distillations of gas condensates and light crude oils were plotted against molecular weight. This figure is reproduced in Figure 5 which plots specific gravity as a function of the carbon number and "aromaticity". Aromaticity was defined as the deviation of the petroleum fraction from n-paraffin behavior. Detailed description of the figure is given by Yarborough[53] and Vogel et al.[47]

The specific gravity curves in Figure 5 were fit using the relationship

$$SG = \frac{0.846 \exp(0.6807\ A) + 0.0003\ C_n}{0.72 \exp(-3.26\ A)\ C_n + 1.2} \qquad (3.14)$$

where A is the aromaticity fraction. The curves in Figure 5 or the relationship above can be used in conjunction with the molecular weight obtained from a GC TBP to yield a density distribution. A match has to be made between the experimental specific gravity of the C_{7+} fraction and the values obtained using Figure 5 or equation 3.14. These curves were also used to obtain the specific gravities of the quadrature pseudo-components in such a way that the mass balance was conserved. A flow chart is shown in Figure 6. In these calculations, an implicit assumption is made that all the pseudo-components have the same aromaticity. It should be noted that the original density curves proposed by Yarborough[53] were up to $C_n = 40$. These have been extrapolated to $C_n = 150$.

3.5 Critical Properties of Quadrature Pseudo-Components:

The critical parameters of petroleum fluids (required by an EOS) are normally not measured experimentally but are calculated through correlations available in the literature. These methods generally correlate

the critical temperature, T_c, critical pressure, P_c, critical volume, V_c, and acentric factor, ω, with the specific gravity, the normal boiling temperature and/or the molecular weight. There are a large number of such correlations available in the literature[54-61]. An excellent review of the available correlations was made by Fu et al.[62-64] They found that the Black and Twu[59] and the Twu[61] correlations performed well for the heavier petroleum fluids.

Based on a review[65] of current literature, the Twu[61] and the Kesler-Lee[57] correlations were selected for estimating the critical properties. These correlations require the specific gravity and either the average boiling temperature or the molecular weight of the component as input. The Twu[61] correlation is applicable for carbon numbers up to approximately 150. Though not used in this study, the correlation developed by Willman and Teja[27] (or any other consistent correlation) can be used for estimating the critical properties for carbon numbers greater than 150.

3.6 Volumetric Calculations:

An EOS can also be used to predict volumetric properties of liquids and fluid mixtures in addition to the phase behavior. However a match of the measured and calculated phase behavior data does not ensure matching the volumetric properties. A two parameter EOS, e.g. PR EOS, does not predict liquid densities accurately. Volume translation methods as those by Peneloux et al.[66] have been used to correct the phase densities while keeping the phase behavior unchanged[67,68]. The main advantage of this method is that the volumetric properties are improved without affecting the phase equilibria calculations.

The method improves volumetric predictions by incorporating a simple translation to the molar volumes in the EOS as follows

$$\tilde{v} = v + c \tag{3.15}$$

where $\tilde{v}$ is the translated or "pseudo-volume", v is the molar volume from an EOS and c is the translation volume. The volume translation method of Peneloux et al[66] was modified by Kokal and Sayegh[69] and this method has been used in the present work. Essentially the Racket equation is used for the "pseudo-volume" and this defines 'c' in equation 3.15. The Racket equation is given by

$$v_s = \frac{R\,T_c}{P_c}\, z_{RA}^{\left(1 + (1 - T_r)^{2/7}\right)} \tag{3.16}$$

where v_s is the molar volume of the saturated liquid, T_c and P_c are the critical temperature and pressure, R is the gas constant, and z_{RA} is the Racket compressibility factor. The Racket equation was used for pure components below their critical temperatures and a constant translation was applied above their critical temperatures. A simple mixing rule was used for the mixture

$$c = \sum x_i\, c_i \tag{3.17}$$

Details of the method are given by Kokal and Sayegh[69].

3.7 Implementation of Semi-Continuous Thermodynamic Approach:

The procedure for phase equilibrium calculations are along the same lines as proposed by Cotterman and Prausnitz[6], Behrens and Sandler[14],

Shibata et al[46]. The molecular weight was selected as the continuous variable. The procedure can be outlined as follows:

1. Selection of a distribution function for the continuous fraction.
2. Fitting or estimating parameters of the distribution function.
3. Assigning pseudo-components corresponding to the Gaussian quadrature points.
4. Estimating the specific gravities, molecular weights and/or the normal boiling points of the quadrature pseudo-components.
5. Calculating the critical properties using correlations.
6. Performing phase equilibria calculations using the EOS with the set of discrete components.
7. Volumetric calculations as outlined in section 3.6 above.

The minimum input required for the continuous fraction is its molecular weight and its composite specific gravity. If these are not available, then they must be evaluated using correlations and other measured quantities. If the molar distribution of the C_{7+} fraction is available, it can be fitted with an analytical distribution function and quadrature determined. In the absence of an analytical distribution function a simple truncated Gauss-Legendre quadrature method can be used. When only the molecular weight and density of the continuous fraction are known, the following procedure was employed:

1. Semi-infinite exponential decay distribution function is used with $\alpha=1$ in equation 3.2. The starting molecular weight of the continuous fraction, I_{min}, is taken to be the molecular weight of the last discrete component plus 7. The value of β is then calculated from

$$\beta = MW_{C_{7+}} - I_{min} \qquad (3.18)$$

2. After the quadrature pseudo-components have been assigned, their specific gravities are obtained using eqn. 3.14 (or Figure 5) in the manner shown in Figure 6.

The effect of using untruncated vs. truncated distribution function was discussed by Behrens and Sandler[14] and Shibata et al.[46]. The reader is referred to their paper for a detailed description for the truncated distribution. Truncation effects dew-point calculations.

CHAPTER 4

RESULTS AND DISCUSSION

The method outlined in previous section was implemented to perform phase equilibrium calculations for a number of different systems. These are described below.

4.1 N-paraffins:

As a first example, a synthetic mixture of paraffins as described by Cotterman and Prausnitz[6] was selected. The molar distribution for the 24 components (C_4-C_{27}) mixture is shown in Figure 7. The molar distribution is described by a gamma distribution with parameters $\alpha = 2.75$, $\beta = 25$ and $I_{min} = 51$.

Using all 24 components, the results for a flash calculation at 500 kPa and 480 K, bubble and dew point calculation at 500 kPa are shown in Table 1. The binary interaction coefficients were all set to zero. The calculations were also performed using both the truncated and untruncated generalized-Gauss-Laguerre (see for example Stroud and Secrest[44]) using 4, 6, 8 and 10 quadrature points. The results are also presented in Table 1. The bubble and dew point temperatures are all within ±2°C. In this particular case the untruncated and truncated distribution schemes did not affect results significantly. For the flash calculation, the mole fraction vaporized is within 0.7% of the 24 components result. It was observed for this case that 6 quadrature points were sufficient to represent the system accurately.

4.2 Gas-Condensate System:

The second examples selected for comparison was a gas-condensate system for which extensive data was reported by Hoffmann et al.[70]. Dew points and flash results were tabulated for the gas-condensate system at 367 K and specific gravities and molecular weights were listed for distillation fractions C_7 through C_{23}. Equilibrium K ratios were also tabulated.

The mixture is considered to be a semi-continuous mixture of discrete hydrocarbons C_1-C_6 and a continuous C_{7+} fraction. Cotterman and Prausnitz[6] considered C_{5+} as the continuous fraction. The C_{7+} fraction properties are given in Table 2. The density data of Hoffmann et al.[70] for the distillation cuts showed some scatter and was fitted using least squares polynomial regression. A six-point quadrature scheme was selected for this case with Γ distribution parameters $\alpha = 1$, $\beta = 45.8$, $I_{min} = 93$ (exponential decay distribution) based on the molecular weight of 138.8.

The binary interaction coefficients, δ_{ij}, used for this system as well as for other systems described below were taken from the literature and were not manipulated. For the C_1-hydrocarbon binaries, the interaction coefficients were reported by Katz and Firoozabadi[71] for use with the Peng-Robinson EOS. They presented a straight line relationship for these interaction coefficients as a function of the heavier hydrocarbon specific gravity. A set of binary interaction coefficients used in this study are presented in Table 3. The results, therefore, which we report here are completely predictive. No effort was made to improve/change the interaction coefficients or alter the critical properties of the components.

Using the six-point quadrature scheme, the calculated dew point was found to be 26.89 MPa at 93.89°C which is slightly higher than the reported value of 26.37 MPa. The calculated liquid composition is compared with the experimental values in Table 4. The dew point pressure was found to be very sensitive to the C_{7+} properties. Hoffmann et al.[70] also reported flash results and gas-oil ratios (GOR) at 6 different pressures. Flash calculations were performed at these pressures and the GORs were computed using the flash and density results. The GORs are compared in Table 5 and the results are plotted in Figure 8. Since the interaction coefficients were not modified, the results are in excellent agreement with experimental data.

Liquid mixture densities were also calculated using the translated Peng-Robinson EOS and the results are shown in Table 6 as well as in Figure 9. The value of z_{RA} for quadrature pseudo-components were calculated using their density data. There is a significant improvement in the density predictions using the translated PR EOS over the original PR EOS.

4.3 Light Oil Systems:

4.3.1 Canadian Light Oil:

The third system selected was a Canadian light oil system described by Wu and Fish[72]. The oil selected for comparison is designated oil number 2 in their paper. The properties of the recombined oil are given in Table 7. A semi-continuous description was used to predict the phase behavior with a hydrocarbon solvent system. The C_{7+} fraction was simulated with 1, 2 and 4 quadrature points. The binary interaction coefficients for C_1-hydrocarbons were those reported by Katz and Firoozabadi[71] as described earlier. The

binary interaction coefficients reported by Mehra[73] were used for the CO_2-hydrocarbon and N_2-hydrocarbon binaries. These values are listed in Table 3. A constant value of 0.1, independent of temperature, was used for CO_2- as well as N_2-C_{7+} pseudo-component binaries. One can also use the Kato[74] correlation for generating the CO_2-hydrocarbon interaction coefficients. This, however, was not done in this study.

The calculated saturation pressures for the recombined oil blended with various concentration of the hydrocarbon solvent using 1, 2 and 4 quadrature points are shown in Figure 10 and tabulated in Table 8. For all three cases the saturation pressure calculations are in good agreement with the experimental values except for the last dew point. The density results using the translated EOS are shown in Figure 11 and listed in Table 9. In this instance the density calculations were performed with a single C_{7+} component. However, similar results were obtained (but not reported) with 2 and 4 quadrature pseudo-components. Finally, the flash results for the recombined oil at 22°C and 89 kPa is presented in Table 10. The match in the GOR and composition is excellent.

It should be noted here that Wu and Fish[72] also reported the prediction results for saturation pressures using the PR EOS with one C_{7+} fraction pseudo-component. They, however, matched the phase behavior results by manipulating the critical properties of the C_{7+} fraction as well as the interaction coefficients between the lighter components with the C_{7+} fraction. The semi-continuous thermodynamic framework of predicting phase equilibria is a much more "scientific" method than that used by Wu and Fish[72].

4.3.2 U.S. Light Oil:

A U.S. light oil system from the Maljamar field in New Mexico was selected as the fourth system. Phase behavior data for this system was reported by Orr et al[75]. The properties of Maljamar separator oil are listed in Table 11. The phase behavior of mixtures of CO_2 and Maljamar separator oil at 32.2°C were predicted using 4 quadrature pseudo-components for the C_{7+} fraction. The interaction coefficients listed in Table 3 were used for the prediction of saturation pressures. The calculated results and smoothed data are plotted in Figure 12. The match between experimental data and calculated results is excellent in the two-phase vapor-liquid and liquid-liquid regions. The three phase L-L-V region was also correctly predicted. However the range of pressures over which the L-L-V region was observed experimentally was larger. Three phase region predictions are extremely sensitive to the critical properties and binary interaction coefficients used and can be improved by altering them. This, however, was not done in this study.

4.4 Heavy Oil Systems

Heavy oils generally contain components with substantially higher molecular masses than those found in conventional or light oil systems. They also contain a higher proportion of aromatics and hetero-atoms than the light oils. This affects the availability of distribution data as experimental techniques for heavy oils are very difficult and often impossible. In a typical simulation distillation experiment (Figure 3) only 40 % of the heavy oil elutes from the GC column and for heavier oils and bitumens, even lower proportions will elute. Without distribution data, the

EOS parameters cannot be evaluated with confidence. Another problem is the determination of critical properties of extremely heavy components due to the limitation of the critical property correlations. Current critical property correlations provide P_c and T_c for carbon numbers up to about C_{100} and their extrapolation to heavier carbon numbers yields ambiguous results.

The limitation of the critical property correlations restricts the application of semi-continuous analysis to very heavy crude oils. Due to the unavailability of critical property correlations for heavy oil components, the number of quadrature points or pseudo-components is limited. In the examples in this study, this was restricted to three quadrature components; for heavier oils, it will be even lower. Fortunately, the number of pseudo-components does not have a significant effect on the phase behavior calculations of the heavy oils. Work on critical property correlations for carbon number up to C_{700} is in progress at the University of Saskatchewan[36].

4.4.1 Lindbergh heavy oil

The first heavy oil system selected was the Lindbergh heavy oil for which the phase behavior data were reported by Sayegh et al.[76]. In that study, phase behavior and physical property measurements were carried out on the heavy oil/CO_2 mixtures at 21°C and 140°C and at pressure ranging up to about 15 MPa. The heavy oil was divided into four fractions: a pentane insoluble fraction comprising resins and asphaltenes, the remaining oil (de-asphalted or De-oil) was further fractionated by distillation into a light, medium and heavy fraction. Experimental measurements were also reported on three of the oil's fractions which serve as pseudo-components

during EOS correlation of the experimental data. Their data is ideal for the present study and can be used to directly compare the quadrature pseudo-components with actual experimental fractions. Sayegh et al.[76] also reported extensive simulated distillation results for the various oil fractions. Some of the fractions eluted only partially from the GC and therefore the oil samples were analyzed for molecular weight distributions using gel permeation chromatography.[77]

The molecular weight distribution of the Lindbergh heavy oil, de-asphalted oil, Fraction 1, Fraction 2 and Fraction 3 is shown in Figure 13. The data was smoothed to even out the random errors without affecting the quality. We tried to fit these distributions to statistical analytical distribution functions but the fit was very poor. The Gauss-Legendre quadrature method was therefore used to obtain pseudo-components and their mole fractions from experimental molecular weight distribution data in Figure 13.

The properties of the Lindbergh heavy oil as well as its fractions is given in Table 12. The molecular weights listed in the table are the average molecular weights of the oil fractions determined from the integration of molar distribution data in Figure 13. These average molecular weights are comparable to the values obtained using vapor pressure osmometry and freezing point determination methods[76]. The molecular weights as well as the distribution data of de-asphalted oil was adjusted slightly to match the overall material balance.

The phase behavior results of CO_2/heavy oil at 21°C are shown in Figure

14 along with the experimental data. Calculations were performed with 1, 2 and 3 quadrature points. All interaction coefficients for CO_2/pseudo-component binaries were taken as 0.1. Both V-L and L-L phase equilibria were observed in this system. A small three phase L-L-V region (in a very narrow range of pressures) was observed during the experiments around the liquefaction pressure of CO_2 (5.88 MPa). This cannot be predicted by an EOS if the heavy oil is considered to be a single component. To correctly predict the observed L-L-V behavior, the crude oil must be characterized by at least two components. With 2 and 3 quadrature components, the L-L-V region was predicted over a narrower range of pressure than that observed experimentally. The curves shift to the right on the composition scale as the quadrature points are increased to 2 and 3. The shift could be adjusted by fine tuning the interaction coefficients. The shift is also reduced as more quadrature points are used. One of the reasons for this shift is the approximate nature of the Gauss-Legendre quadrature method used. Finally the heavy oil phase behavior is also predicted using two components: De-oil and asphaltenes with the experimental mole fractions and molecular weights. The dashed curve in Figure 14 falls on top of the dotted curve for two quadrature components. This shows the rather insensitive nature of the splitting process of the heavy oil into fractions on the phase behavior calculations.

The results for CO_2/De-oil mixtures at 21°C are shown in Figure 15. The shift of the curves with the numbers of quadrature components is less than that of the heavy oil. The dashed curve in Figure 15 represents the predictions using a three component system containing Fraction 1, Fraction 2 and Fraction 3 with experimental split compositions. The curve lies very

close to the curve for the three quadrature points.

Predicted phase behavior results for CO_2/Fraction 2 mixtures at 21°C are presented in Figure 16. The deviation in composition with quadrature points at a given pressure (in the L-L region) is much less than that in either the De-oil or the heavy oil cases. The reason for this is the fact that the Gauss-Legendre quadrature method was found to be more accurate for the low molecular weight fluids. The match for the bubble points is excellent considering the fact that this is a prediction without altering any adjustable parameters.

The phase behavior results of CO_2/Fraction 1 mixture at 21°C are shown in Figure 17. This system exhibits V-L equilibrium only and the point at 8.27 MPa was in the single phase region. The three curves for the 1, 2 and 3 quadrature points are virtually on top of each other and the match with the experimental data is good.

The predicted results and experimental data for the Lindbergh heavy oil, De-oil, Fraction 1 and Fraction 2 at 140°C using 1, 2 and 3 quadrature points are shown in Figures 14 to 17. In all cases the predicted results lie to the left of the experimental data points, suggesting that a constant value of 0.1 for the interaction coefficients is probably not adequate at this temperature. Kokal and Sayegh[65] found the interaction coefficients for this system to be temperature dependent. One could also use the Kato[74] correlation for predicting the interaction coefficients for the CO_2/oil systems.

The predicted results using the PR and the translated PR EOS (designated PRT) for mixtures of CO_2 with the heavy oil, De-oil, Fraction 2 and Fraction 1 at 21°C are shown in Figures 18 to 21. respectively. The values of the Racket compressibility factor for the oils were calculated using experimental density data at 21°C and 140°C. Figures 18 to 21 show the superior density results of the translated PR EOS. For all systems except Fraction 1, the errors in the density predictions using the translated PR EOS were less than 1% while for the PR EOS the overall absolute percent errors were in the 18 to 22 % range. These results were calculated using only 1 quadrature component. However the match was found to be excellent even for 2 and 3 quadrature pseudo-components. Details of the density correlation are provided by Kokal and Sayegh[69]. The density results at 140°C for the various oils saturated with CO_2 are also shown in Figures 18 to 21; again the improvements in the saturated liquid densities are large. From these figures it is also evident that the translation method correctly predicts the trends in the densities with pressure eg. densities increase with pressure at 21°C and decrease with pressure at 140°C.

4.4.2 Lone Rock Heavy Oil

The second heavy oil system selected was from the Lone Rock field in western Saskatchewan. It has a viscosity of 2000 mPa.s and a density of 950 kg/m^3 at room temperature which makes it somewhat lighter than the Lindbergh crude oil. The phase behavior and physical property data were measured by Kokal et al.[78]. The heavy oil was divided into three fractions: a pentane insoluble asphaltene/resin fraction and the de-asphalted oil (De-oil) which was further distilled into a light (F_1) and a heavy (F_2)

fraction. Phase behavior and physical property measurements are reported on mixtures of CO_2 with the heavy oil, De-oil, F_2 and F_1. The molecular weight distributions of the various fractions were also obtained[77] by GPC and are plotted in Figure 22. The properties of the Lone Rock heavy oil as well as its fractions are given in Table 13. As with the Lindbergh heavy oil system, the molecular weight of the Lone Rock De-oil was also adjusted to match the overall material balance.

The phase behavior results for mixtures of CO_2 with the heavy oil, De-oil, F_2 and F_1 are shown in Figures 23 to 26 using 1, 2 and 3 quadrature components at 21°C and 140°C along with the experimental data. The results are similar to the Lindbergh heavy oil system.

Excellent results were also obtained for the mixture liquid densities using the translated PR EOS and the results are shown in Figure 27 to 30 for the heavy oil, De-oil, F_2 and F_1 at 21°C and 140°C.

CHAPTER 5

CONCLUSIONS

1. The semi-continuous thermodynamic description coupled with an EOS can be used effectively to model the phase behavior of solvent/crude oil systems.
2. Continuous thermodynamics has several advantages over the conventional pseudo-component method and avoids the "trial-and-error" procedure and arbitrariness in the definition of pseudo-components. It also reduces computational time requirements without affecting accuracy.
3. Untruncated (open) semi-infinite distribution functions eg. Γ distribution function affects dew point calculations and may not be suitable in some situations. Truncated (closed) distribution as described by Behrens and Sandler[14] and Shibata et al.[46] can be used in those cases. Alternatively the closed distribution function can be obtained from experimental data by means of spline fit and normalization.
4. The semi-continuous thermodynamic description presently is restricted due to limitations of the critical property correlations for very heavy components. Work on this aspect is in progress[36].
5. The use of binary interaction coefficients as a correlating factor should be used with caution since they may not have physical significance when used without restraint. A concerted effort is needed to obtain generalized interaction coefficients for equations of state especially for solvent/crude oil systems.
6. Complete and extensive sets of experimental data on the phase behavior of heavy oil systems to further test the continuous thermodynamic

concepts is urgently required.

7. Significant improvements in saturated liquid density predictions can be achieved by using the volume translated PR EOS and the Racket equation. The PR EOS density prediction errors for the heavy oil mixtures were in the 18-20 % range and were less than 1-2 % for the translated PR EOS.

REFERENCES

1. Briano, J. and Glandt, E.D., "Molecular Thermodynamics of Continuous Mixtures", Fluid Phase Equilibria, v. 14, p. 91-102 (1983).

2. Gal-Or, B., Cullinan Jr., H.T., Galli,R., "New Thermodynamic-Transport Theory for Systems with Continuous Component Density Distributions", Chem. Eng. Sci., v. 30, p. 1085 (1975).

3. Gualtieri, J.A., Kincaid, J.M. and Morrison, G., "Phase Equilibria in Polydisperse Fluids", J. Chem. Phys., v. 77, p. 521 (1982).

4. Kehlen, H., Ratzsch, M. T., and Bergmann, J., "Continuous Thermodynamics of Multicomponent Systems", AIChE J., v. 31, n. 7, pp. 1136-48 (1985).

5. Ratzsch, M.T. and Kehlen, H., "Continuous Thermodynamics of Complex Mixtures", Fluid Phase Equilibria, v. 114, p. 225-234 (1983).

6. Cotterman, R.L. and Prausnitz, J.M., "Flash Calculations for Continuous or Semi-continuous Mixtures Using an Equation of State", IEC Proc. Des. Dev., v. 24, pp. 434-443 (1985).

7. Cotterman, R.L., Bender, R., and Prausnitz, J.M., "Phase Equilibria for Mixtures Containing Very Many Components. Development and Application of Continuous Thermodynamics for Chemical Process Design", Ind. Eng. Chem. Fund., v. 24, pp. 194-203 (1985).

8. Du, P.C., Mansoori, G.A., "Phase Equilibrium Computational Algorithms of Continuous Mixtures", Fluid Phase Equilibria, v. 30, p. 57 (1986).

9. Prausnitz, J.M., "Phase Equilibria for Complex Fluid Mixtures", Fluid Phase Equilibria, v. 14, pp. 1-18 (1983).

10. Chou, G.F. and Prausnitz, J.M., "Adiabatic Flash Calculations for

Continuous or Semi-Continuous Mixtures Using and Equation of State", Fluid Phase Equilibria, v. 30, pp. 75-82 (1986).

11. Angelos, C.P. and Ewing, R.E., "Continuous Thermodynamic Correlations for Thermal Simulations Using a Cubic Equation of State", AIChE Symposium Series - Heat Transfer, pp. 186-190 (1988).

12. Kehlen, H. and Ratzsch, M.T., "Complex Multicomponent Distillation Calculations by Continuous Thermodynamics", Chem. Eng. Sci., v. 42, pp. 221-232 (1987).

13. Kehlen, H., Ratzsch, T., Ruzicka, V. Jr., and Sadowski, G., "Continuous Thermodynamics of the Liquid-Liquid Equilibrium for Systems Containing Petroleum Fractions ", Z. Phys. Chem. (Leipzig), v. 269, n. 5, pp. 908-16 (1988).

14. Behrens, R.A., Sandler, S.I., "Use of Semicontinuous Description to Model the C7+ Fraction in Equation-of-State Calculations", SPE Reservoir Engineering, v. 3, n. 3, p. 1041 (1988).

15. Du, P.C. and Mansoori, G.A., "A Continuous Mixture Computational Algorithm for Reservoir Fluids Phase Behavior", paper SPE 15082, presented at the California Regional Meeting, Oakland, CA, April 2-4 (1986).

16. Du, P.C., Mansoori, G.A., "Continuous Mixture Computational Algorithm of Reservoir Fluid Phase Behavior Applicable for Compositional Reservoir Simulation", Paper no. SPE 15953, presented at the SPE Eastern Regional Meeting, Columbus, Ohio, Nov. 12-14, (1986).

17. Peng, D.-Y., Wu, R.S., and Batycky, J.P., "Application of Continuous Thermodynamics to Oil Reservoir Fluid Systems Using an Equation of State", AOSTRA J. of Research, v. 3, pp. 113-122 (1987).

18. Ying, X., Ye, R., and Hu, Y., "Phase Equilibria for Complex Mixtures. Continuous Thermodynamics Based on Spline Fit", Fluid Phase

Equilibria, v. 53, pp. 407-414, (1989).

19. Halpin, T.P.J. and Quirke, N., " A New Method of Continuous Thermodynamics Applied in an Equation of State", SPE unsolicited paper no. 18722, (1988).

20. Ratzsch, M.T., Kehlen, H., and Schumann, J., "Flash Calculations for a Crude Oil By Continuous Thermodynamics", Chem. Eng. Commun., v. 71, pp. 113-25 (1988).

21. Wang, S.H. and Whiting, W.B., "A Group-Contribution, Continuous-Thermodynamics Framework for Calculation of Vapor-Liquid Equilibria", Can. J. Chem. Eng., v. 65, n. 4, pp. 651-661 (1987).

22. Radosz, M., Cotterman, R.L., and Prausnitz, J.M, "Phase Equilibria in Supercritical Propane Systems for Separation of Continuous Oil Mixtures", IEC Res., v. 26, pp. 731-737 (1987).

23. Salacuse, J.J. and Stell, G., "Polydisperse Systems: Statistical Thermodynamics with Application to Several Models Including Hard and Permeable Spheres", J. Chem. Phys., v. 77, n. 7, pp. 3714-3725 (1982).

24. Gutsche, B., "Phase Equilibria in Oleochemical Industry - Application of Continuous Thermodynamics", Fluid Phase Equilibria, v. 30, pp. 65-73 (1986).

25. Moore, P.K. and Anthony, R.G., "Continuous Equilibrium Calculations - A Discrete Approach", Paper no. 19f, presented at the AIChE Spring National Meeting and Petro Expo, Houston, TX, March 29 - April 2, (1987).

26. Schlyper, A.G., "Flash Calculations for Polydisperse Fluids: A Variational Approach", Fluid Phase Equilibria, v. 34, pp. 149- 169 (1987).

27. Willman, B. and Teja, A.S., "Continuous Thermodynamics of Phase

Equilibria Using a Multivariate Distribution Function and an Equation of State", AIChE J., v. 32, pp. 2067-2078 (1986).

28. Abbasian, M..J., Weil, S.A., "Phase Equilibria of Continuous Fossil Fuel Process Oils", AIChE J., v. 34, n. 4, p. 574 (1988).

29. Cotterman, R. L., Prausnitz, J.M., "Continuous Thermodynamics for Enhanced Oil Recovery. High-Pressure Phase Equilibria for Reservoir Simulation", Proceedings of the Third European Meeting on Improved Oil Recovery, Rome, pp. 39.47, Apr.16-18, (1985).

30. Ratzsch. M.T., Kehlen, H., and Baumann, F., "Application of Continuous Thermodynamics to the Vapor-Liquid Equilibrium of Complex Hydrocarbon Mixtures", Z. Phys. Chem. (Leipzig), v. 268, n. 3, pp. 614-18 (1987).

31. Cotterman, R.L. , "Phase Equilibria for Complex Fluid Mixtures at High Pressures. Development and Application of Continuous Thermodynamics ", Ph.D. Dissertation, University of California, Berkley (1986).

32. Cotterman, R.L., Dimitrelis, D., and Prausnitz, J.M., "Supercritical Extraction Calculations for High-Boiling Petroleum Fractions Using Propane. Application of Continuous Thermodynamics", Ber. Bunsen. Physik. Chem., v. 88, n. 9, pp. 796-801 (1984).

33. Cotterman, R.L., Dimitrelis, D., and Prausnitz, J.M. , "Design of Supercritical-Fluid-Extraction Processes Using Continuous Thermodynamics", Process Technol. Proc. (PTPREM), v. 3 (Supercrit. Fluid Technol.), pp. 107-20 (1985).

34. Willman, B.T., "Continuous Thermodynamics of Fluid Mixtures", Ph.D. Dissertation, Univerty of Georgia, Georgia, (1986)

35. Teja, A.S. and Willman, B.T., " Phase Equilibria in Natural Gas, Crude Oil and Coal Liquid Mixtures", Fluid Phase Equilibria, v. 30, pp. 247-253 (1986).

36. Peng, D-Y., "Continuous Thermodynamics for Bitumens and Heavy Oils", 13th Annual AOSTRA/University/Industry Technical Review Meeting and Seminar, Banff, Alberta, October 12-14, (1988).

37. Willman, B. and Teja, A.S., "Prediction of Dew Points of Semicontinuous Natural Gas and Petroleum Mixtures. 1. Characterization by Use of an Effective Carbon Number and Ideal Solution Predictions", Ind. Eng. Chem. Res., v. 26, p. 948 (1987).

38. Willman, B. and Teja, A.S., "Prediction of Dew Points of Semicontinuous Natural Gas and Petroleum Mixtures. 2. Non-ideal Solution Calculations", Ind. Eng. Chem. Res., v. 26, p. 953 (1987).

39. Won,K.W., "Continuous Thermodynamics for Solid-Liquid Equilibria. Wax Formation from Heavy Hydrocarbon Mixtures", Presented at 1985 AIChE Spring National Mtg., Houston, TX, Mar.23-26, (1985).

40. Kawanaka, S., Park, S.J., Mansoori, G.A., "The Role of Asphaltene Deposition in EOR Gas Flooding: A Predictive Technique", Paper no. 17376, Proceedings of SPE/DOE Sixth Symposium on Enhanced Oil Recovery, Tulsa, OK, April 17-29, (1988).

41. Peng, d.-Y. and Robinson, D.B., "A New Two-Constant Equation of State", Ind. & Eng. Chem. Fundamentals, v. 15, n. 1, pp. 59-64 (1976).

42. Ratzsch, M.T., Kehlen, H., and Baumann, F., "Application of Continuous Thermodynamics to the Vapor-Liquid Equilibrium of Complex Hydrocarbon Mixtures", Z. Phys. Chemie (Leipzig), v. 268, pp. 614-618 (1987).

43. Ratzsch, M.T. and Kehlen, H., "Equilibrium Flash Vaporization Curves By Continuous Thermodynamics", Z. Phys. Chem. (Leipzig), v. 266, n. 2, pp. 329-39 (1985).

44. Stroud, A.H. and Secrest, D., *Gaussian Quadrature Formulas*, Prentice-Hall, Englewood Cliffs, NJ, (1966).

45. Whitson, C.H., "Characterizing Hydrocarbon Plus Fractions", SPE J., pp. 683-694, (1983).

46. Shibata, S.K., Sandler, S.I. and Behrens, R.A., "Phase Equilibrium Calculations for Continuous and Semicontinuous mixtures", Chem. Eng. Sci., v. 42, n. 8, pp 1977-1988, (1987).

47. Vogel, J.L., Turek, R.S., Bergman, D.F. and Morris, R.W., "Applications of Equations of State to Calculate Reservoir Fluid Properties", Fluid Phase Equilibria, pp 103-116, v. 14, (1983).

48. Walpole, R.E. and Myers, R.H., *Probability and Statistics for Engineers and Scientists*, Macmillan Inc., New York, (1985).

49. Cotterman, R.L., Chou, G.F. and Prausnitz, J.M., "Comments on 'Flash Calculations for Continuous or Semicontinuous Mixtures Using an Equation of State'", Ind. Eng. Chem. Process Des. Dev., v. 25, pp 840-841, (1986).

50. Leontaritis, K.J. and Mansoori, G.A., "Use of High Performance Liquid Chromatography and Gel Permeation Chromatography for Characterization of Resins and Asphaltenes", Int. J. Pet. Sci. Eng., v. 2, pp. 1-12, (1989).

51. Champagne, P.J., Manolakis, E. and Ternan, M., "Molecular Weight Distribution of Athabasca Bitumen", Fuel, v. 64, pp. 423-425, (1985).

52. Long, R.B., "The Concept of Asphaltenes", in *Chemistry of Asphaltenes*, (eds. J.W. Bunger and N.C. Li), American Chemical Society, Advances in Chemistry Series, v. 195, pp. 17-27, (1981).

53. Yarborough, L. "Application of a Generalized Equation of State to Petroleum Reservoir Fluids", in *Equations of States in Engineering*, (eds. K.C. Chao and R.L. Robinson, Jr.), Advances in Chemistry Series, American Chemical Society, pp. 385-435, (1979).

54. Cavett, R.H., "Physical Data for Distribution Calculations - Vapor-Liquid Equilibrium", Proc. 27th API Meeting, San Francisco, (1962).

55. Smith, R.L. and Watson, K.M., "Boiling Points and Critical Properties of Hydrocarbon Mixtures", Ind. Eng. Chem., v. 29, pp. 1408-1414, (1937).

56. Watson, K.M. and Nelson, E.F., " Improved Methods for Approximating Critical and Thermal Properties of Petroleum Fractions", Ind. Eng. Chem., v. 25, pp. 880-887, (1933).

57. Kesler, M.G. and Lee, B.I., "Improve Predictions of Enthalpy of Fractions", Hydrocarbon Processing, pp. 153-158, (1976).

58. Riazi, M.R. and Daubert, T.E., "Simplify Property Predictions", Hydrocarbon Processing, pp.115-116, (1980).

59. Black, C. and Twu, C.H., "Correlation and Prediction of Thermodynamic Properties for Heavy Petroleum, Shale Oils, Tar Sands and Coal Liquids", Paper presented at AIChE 1983 Spring National Meeting, Houston, Texas, (1983).

60. Twu, C.H., "Prediction of Thermodynamic Properties of Normal Paraffins Using only Normal Boiling Point", Fluid Phase Equilibria, v. 11, pp. 65-81, (1983).

61. Twu, C.H., "An Internally Consistent Correlation for Predicting the Critical Properties and Molecular Weight of Petroleum and Coal Tar Liquids", Fluid Phase Equilibria, v. 16, pp. 137-150, (1984).

62. Fu, C.-T., Puttagunta, V.R. and Pors, D., "Estimation Methods for Pseudo-Critical Properties of Heavy Hydrocarbons", AOSTRA/ARC Joint Report, Oil Sands Index # 8586-49, Edmonton, Canada, (1986).

63. Fu, C.-T., Puttagunta, V.R., Baumber, L. and Hsi., C.,

"Pseudo-Critical Properties of Heavy Oils and Bitumen", Fluid Phase Equilibria, v. 30, pp. 281-295, (1986).

64. Fu, C.-T., Puttagunta, V.R. and Hsi., C., "Sensitivities in Representing the Phase Behavior of Gas-Bitumen Systems", Can. J. Chem. Eng., v. 65, pp. 208-313, (1987).

65. Kokal, S.L. and Sayegh, S.G., "Phase Behavior Correlation of CO_2/Heavy Oil Mixtures for Enhanced Oil Recovery", Fluid Phase Equilibria, v. 52, pp. 283-290, (1989).

66. Peneloux, A., Rauzy, E. and Freeze, R., "A Consistent Correction for Redlich-Kwong-Soave Volumes", Fluid Phase Equilibria, v. 8, pp. 7-23, (1982).

67. Jhaveri, B.S. and Youngren, G.K., "Three-Parameter modification of the Peng-Robinson Equation of State to Improve Volumetric Predictions", SPE Reservoir Engineering, pp. 1033-1040 (1988).

68. Deo, M.D., Nuttaki, R., and Orr Jr., F.M., "Schmidt-Wenzel and Peng-Robinson Equations of State for CO_2-Hydrocarbon Mixtures: Binary Interactions Parameters and Volume Translation Factors", SPE paper 18976 presented at the SPE California Regional Meeting, (1989).

69. Kokal, S.L. and Sayegh, S.G., "Gas-Saturated Bitumen Density Predictions Using the Volume Translated Peng-Robinson Equation of State", paper accepted for publication in J. Can. Petrol. Tech., (1990).

70. Hoffmann, A.E., Crump, J.S. and Hocott, C.R., "Equilibrium Constants for a Gas-Condensate System", Petroleum Trans. AIME, v. 198, pp. 1-10, (1953).

71. Katz, D.L. and Firoozabadi, A., "Predicting Phase Behavior of Condensate/Crude-Oil Systems Using Methane Interaction Coefficients", J. Petrol. Tech., pp. 1649-1655, (1978).

72. Wu, R.S. and Fish, R.M., "C_{7+} Characterization for Fluid Properties Predictions", J. Can. Petrol. Tech., v. 28, n. 4, pp 112-117, (1989).

73. Mehra, R.K., "The Computation of Multi-phase Equilibrium in Compositional Reservoir Studies", PhD. Dissertation, University of Calgary, (1981).

74. Kato, K., "Generalized Interaction Parameters for the PR EOS: CO_2/n-Paraffin Binary System", Fluid Phase Equilibria, v. 7, pp. 219-231, (1981).

75. Orr, F.M., Yu, A.D., and Lien, C.L., "Phase Behavior of CO_2 and Crude Oil in Low-Temperature Reservoirs", SPE J., pp. 480-492, Aug. (1981).

76. Sayegh, S.G., Rao, D.N., Kokal, S.L. and Najman, J., "Phase Behavior and Physical Properties of Lindbergh Heavy Oil/CO_2 Mixtures", paper n. 89-40-45, presented at the 40th Annual Technical Meeting of the Petroleum Society of CIM, Calgary, Alberta, 28-31 May (1989), accepted for publication in the J. Can. Pet. Tech.

77. Coulombe, S., "Determination of Molecular Weight Distribution of Crude Oils and Their Fractions", Energy Research Laboratories Division Report ERL 90-12, submitted to PRI, Feb. (1990).

78. Kokal, S.L., Najman. J., and Sayegh, S.G., "Phase Behavior and Physical Properties of CO_2/Heavy Oil Mixtures for Enhanced Oil Recovery", submitted to UNITAR/UNDP Fifth International Conference on Heavy Crude and Tar Sands, Caracas, Venezuela, February (1990).

Table 1: Sensitivity results for 24 components n-paraffin example at 500 kPa

Quadrature method	Bubble Point (C)	Dew Point (C)	Flash at 480 K mole fraction vaporized
24 components	157.65	266.17	0.5952
Untruncated			
1. 4-point	159.50	266.47	0.5979
2. 6-point	158.82	266.47	0.5966
3. 8-point	158.76	266.36	0.5976
4. 10-point	158.75	266.44	0.5971
Truncated			
1. 4-point	159.38	266.02	0.5995
2. 6-point	158.80	266.42	0.5961
3. 8-point	158.76	266.48	0.5975
4. 10-point	158.76	266.43	0.5969

Table 2: Hoffmann et al.[70] reservoir gas composition

Component	Mole %
C_1	91.35
C_2	4.03
C_3	1.53
C_4	0.82
C_5	0.34
C_6	0.39
C_{7+}	1.54

$MW_{C7+} = 138.78$

$\rho_{c7+} = 792.12$ kg/m^3

Table 3: Binary interaction coefficients used in this study

Component	CO_2	N_2	C_1	C_2
CO_2	-	0.0	0.10	0.125
N_2	0.0	0.0	0.036	0.09
C_1	0.10	0.036	0.0	0.0
C_2	0.125	0.09	0.0	0.0
C_3	0.125	0.10	0.0	0.0
C_4	0.125	0.10	0.02	0.0
C_5	0.125	0.10	0.02	0.0
C_6	0.125	0.10	0.025	0.0
C_{7+}	0.10	0.10	#	0.01

#using Katz and Firoozabadi[71] correlation

Table 4: Dew point results for a reservoir gas mixture of Hoffmann et al.[70] at 93.9°C

Component	← Mole % → Vapor (feed)	Liquid expt.	Liquid calc.
C_1	91.35	52.00	53.22
C_2	4.03	3.81	4.28
C_3	1.53	2.37	2.42
C_4	0.82	1.72	1.79
C_5	0.34	1.20	1.07
C_6	0.39	2.06	1.77
C_{7+}	1.54	36.84	25.45

Calculated dew point pressure = 26.89 MPa

Experimental dew point pressure = 26.4 MPa

Table 5: Gas-oil ratios for a reservoir gas mixture of Hoffmann et al.[70] at 93.9°C

Pressure (MPa)	GOR (m^3/m^3) Expt.	Calc.
3.55	11807	11922
7.00	11511	10779
10.45	10491	10811
13.89	11449	11803
17.34	14321	14240
20.10	19639	18478

Vapor volumes at 15.5°C and 101.325 kPa

Table 6: Comparison of liquid mixture densities for flashed reservoir gas mixture of Hoffmann et al.[70] at 93.9°C

Pressure (MPa)	Expt. (kg/m^3)	PR* (kg/m^3)	PRT* (kg/m^3)
3.55	720.9	663.8	722.1
7.00	716.0	646.5	699.1
10.45	675.3	630.8	681.8
13.89	653.8	616.6	667.9
17.34	653.6	603.8	656.6
20.10	656.5	594.6	649.1
27.00	650.0	575.0	635.0

*Original PR EOS; *Translated PR EOS

Table 7: Properties of oil # 2 and hydrocarbon solvent of Wu & Fish[72]

Component	Reservoir fluid	Solvent
N_2	1.98	4.70
CO_2	0.07	0.00
C_1	27.06	51.80
C_2	8.20	15.70
C_3	7.90	14.30
C_4	6.74	9.00
C_5	4.84	2.60
C_6	3.07	1.70
C_{7+}	40.14	

C_{7+} MW = 202

C_{7+} density = 840.0 kg/m^3

Table 8: Comparison of saturation pressures for oil # 2 of Wu and Fish[72] at 62°C

Solvent (mole %)	Saturation pressures in MPa			
	Expt.	1Q*	2Q	4Q
0	12.40	12.25	11.98	12.03
10		13.85	13.54	13.61
20	16.27	15.53	15.19	15.29
30		17.29	16.92	17.06
40	18.81	19.09	18.72	18.94
50		20.89	20.58	20.90
60	22.06	22.57	22.46	22.93
70		23.89	24.39	24.93
80	24.48	24.34	26.49	26.62

*Quadrature point

Table 9: Comparison of saturated liquid densities for oil # 2 of Wu and Fish[72] at 62°C

Pressure MPa	Liquid Density in kg/m^3				
	Expt.	PR	1Q	2Q	4Q
12.00		649.3	701.3	699.9	701.1
13.10	700.9	650.0	701.6	700.9	702.1
13.79	701.7	650.8	702.2	701.5	702.7
14.48	702.6	651.7	702.7	702.1	703.3
15.86	704.3	653.3	703.8	703.2	704.4
17.24	705.9	654.8	704.8	704.3	705.5
18.62	707.5	656.4	705.9	705.4	706.5
20.68	709.9	658.5	707.3	706.9	708.0
23.00		660.8	708.8	708.5	709.6

Table 10: Comparison of flashed gas and liquid composition for oil # 2 of Wu and Fish[72] at 22°C

Component	Reservoir fluid	Experimental		Calculated	
		Gas	Liquid	Gas	Liquid
N_2	1.98	3.80	0.00	3.80	0.01
CO_2	0.07	0.12	0.00	0.12	0.00
C_1	27.06	51.77	0.05	51.77	0.21
C_2	8.20	15.49	0.23	15.33	0.43
C_3	7.90	14.03	1.19	13.75	1.54
C_4	6.74	9.70	3.47	9.62	3.61
C_5	4.84	4.05	5.63	4.29	5.43
C_6	3.07	1.04	6.36	1.09	5.23
C_{7+}	40.14	0.00	83.07	0.28	83.54
GOR (m^3/m^3)		140		130	

Table 11: Properties of Maljamar separator oil

Density at 15.5°C:	829.4 kg/m^3
Viscosity at 34.4°C:	2.8 mPa.s
Molecular Weight:	183.7
Molecular weight of C_{7+}:	199.3
Density of C_{7+} at 15.5°C:	844.1 kg/m^3

Table 12: Properties of Lindbergh heavy oil and its fractions

Component	MW	ρ kg/m^3	Wt. % HO	Wt. % De-oil	Mole % HO	Mole % De-oil
Heavy Oil	470	968				
Solids	1285	1048	28		10.2	
De-oil	377	940	72		89.8	
F_1	169	821		9.6	19.2	21.4
F_2	227	907		23.2	34.7	38.6
F_3	633	972		67.2	35.9	40.0

Table 13: Properties of Lone Rock heavy oil and its fractions

Component	MW	ρ kg/m^3	Wt. % HO	Wt. % De-oil	Mole % HO	Mole % De-oil
Heavy Oil	404	950				
Solids	1336	1060	20		6.1	
De-oil	344	926	80		93.9	
F_1	179	834		19.6	35.7	38.0
F_2	446	952		80.4	58.2	62.0

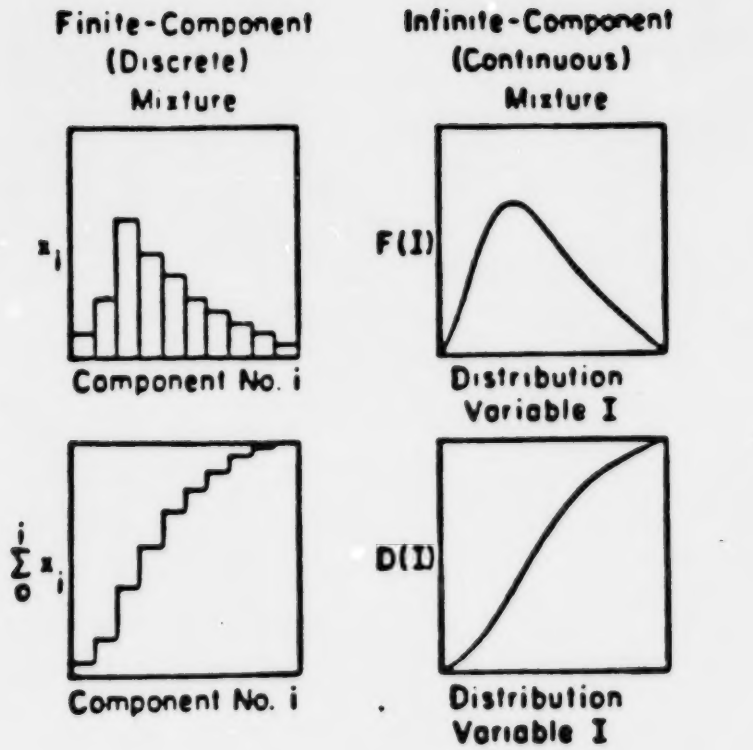

$$\sum_{\text{all } i} x_i = 1.0 \qquad D(I=\infty) = \int_0^\infty F(I)dI = 1.0$$

x = Mole Fraction F = Distribution Function

I is a characterizing quantity, e.g., molecular weight.

FIGURE 1

(REFERENCE 6)

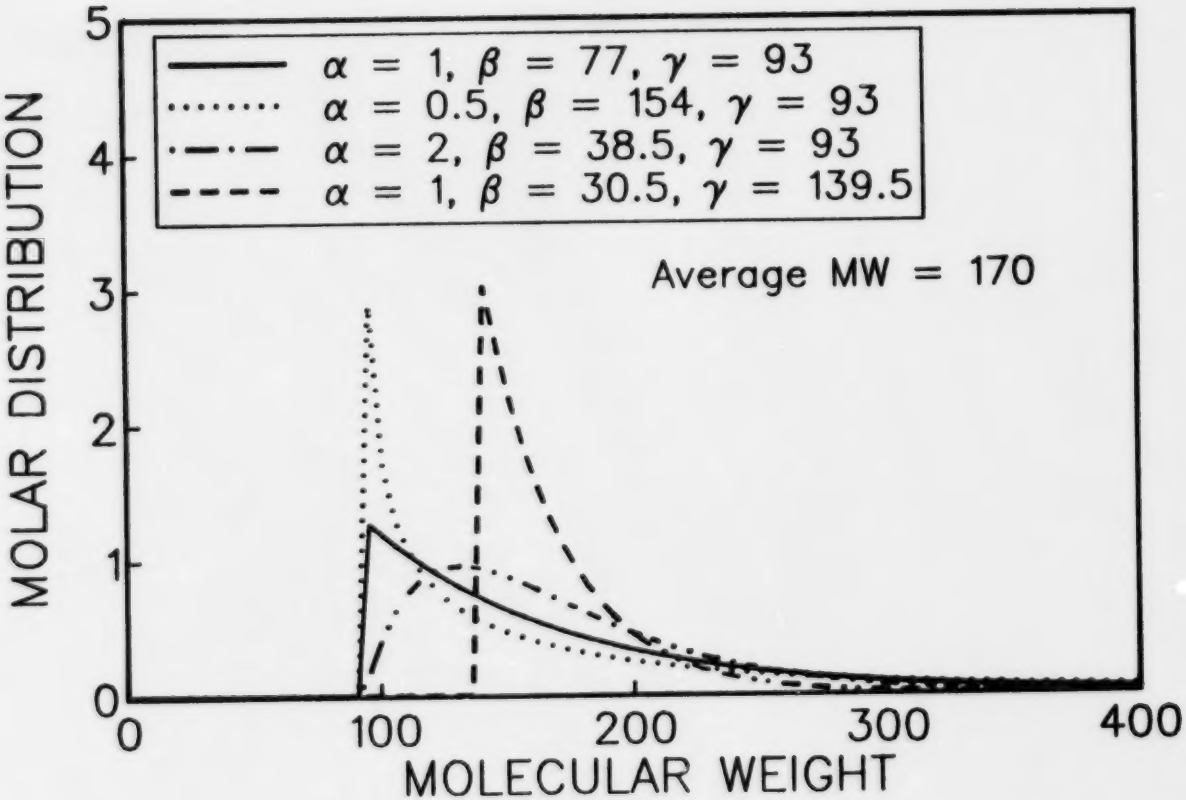

The Γ density distribution function
Effect of distribution parameters

FIGURE 2

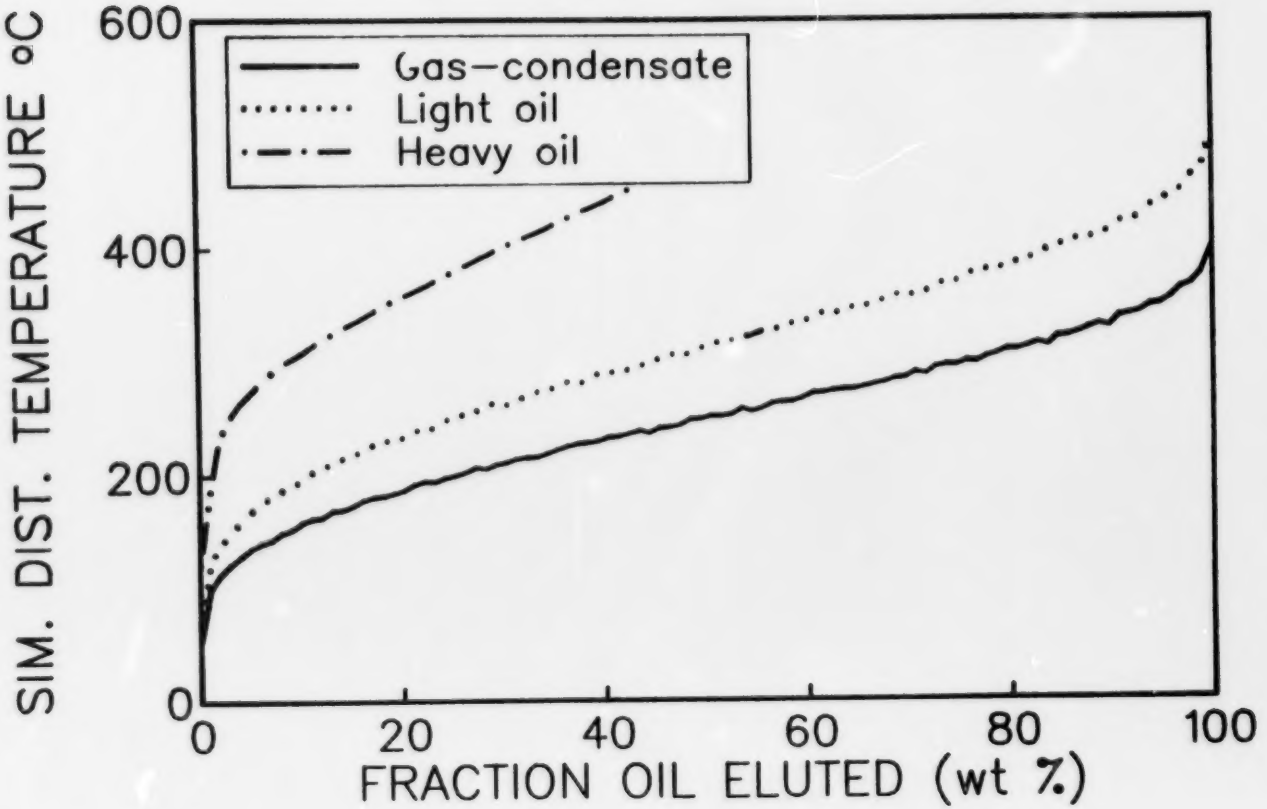

Gas–Chromatograph simulated distillation curves for typical petroleum fluids

FIGURE 3

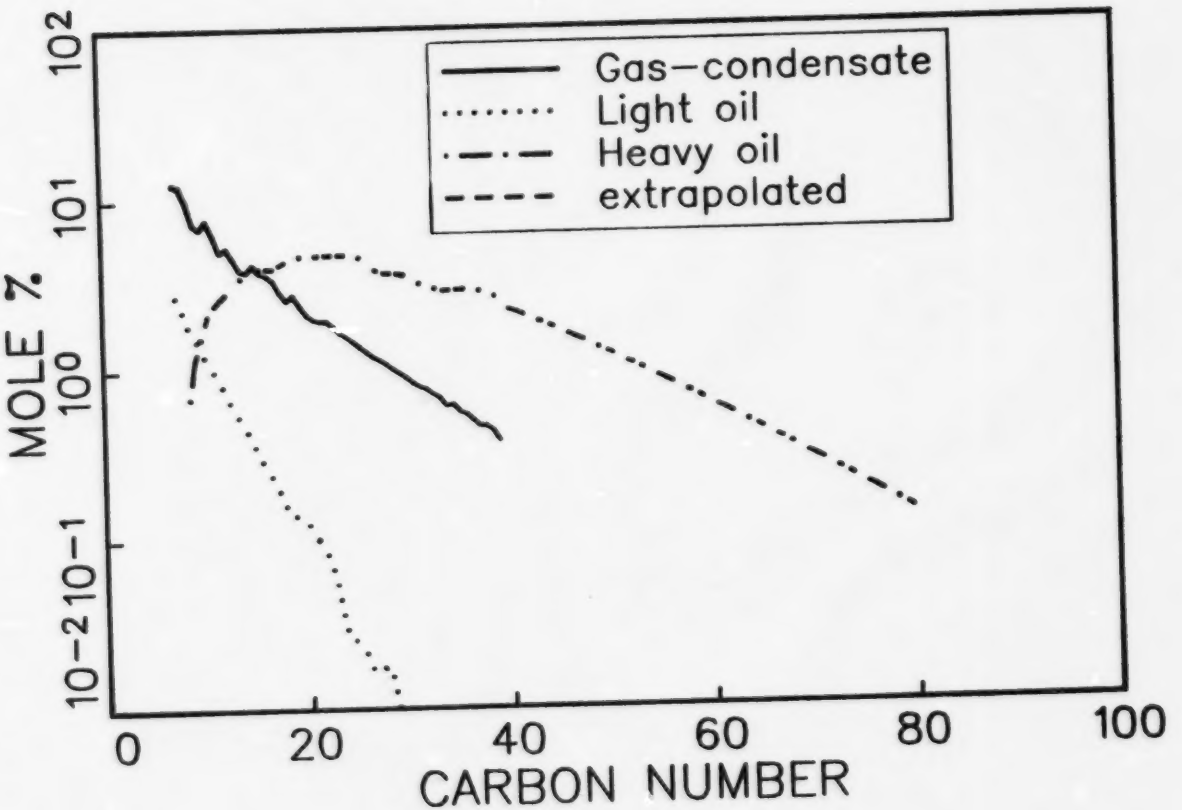

Typical molar distribution using
Gas–Chromatograph simulated distillation

FIGURE 4

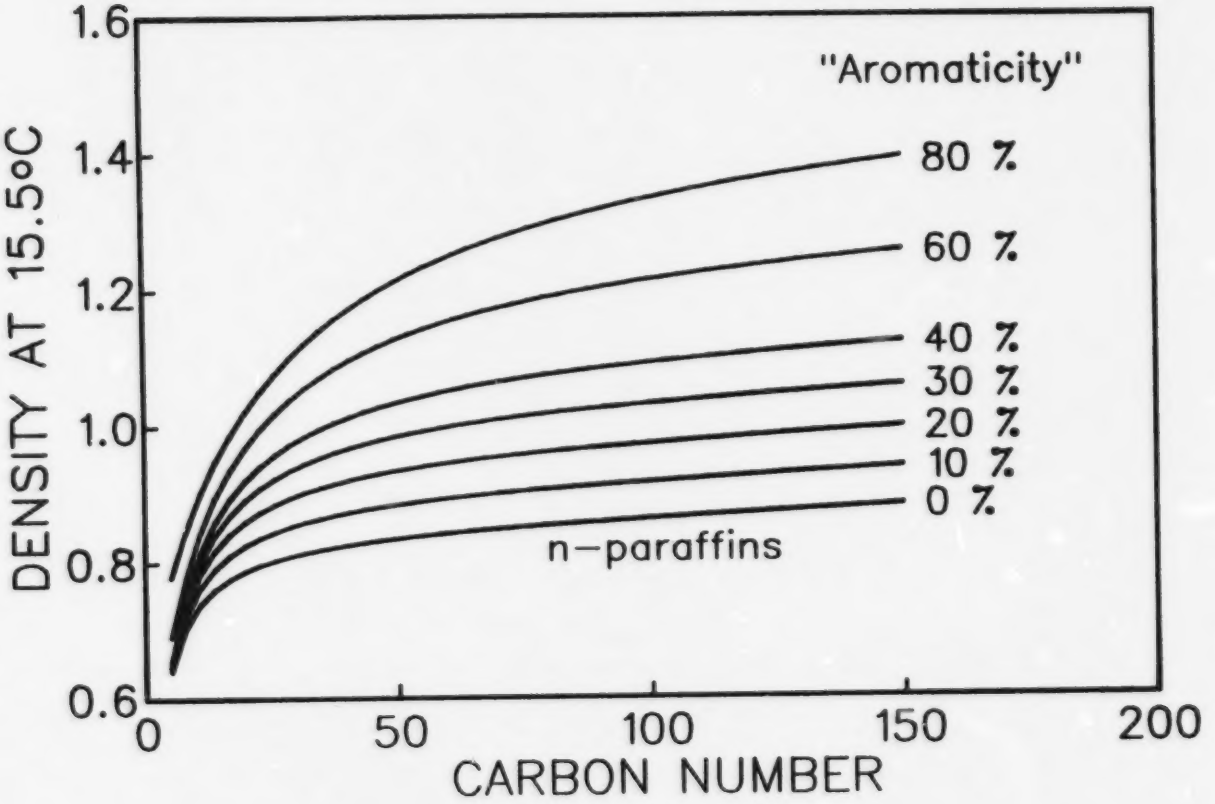

Density curves as a function of carbon number and aromaticity

FIGURE 5

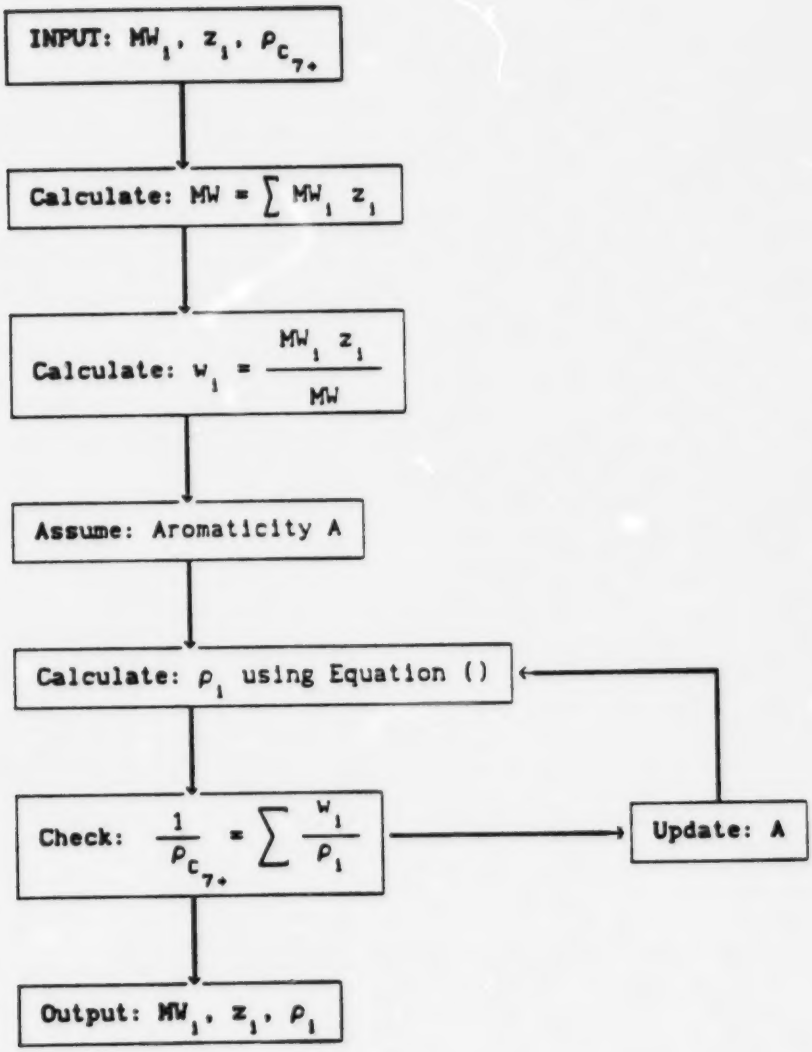
INPUT: MW_i, z_i, $\rho_{C_{7+}}$
Calculate: $MW = \sum MW_i z_i$
Calculate: $w_i = \frac{MW_i z_i}{MW}$
Assume: Aromaticity A
Calculate: ρ_i using Equation ()
Check: $\frac{1}{\rho_{C_{7+}}} = \sum \frac{w_i}{\rho_i}$
Update: A
Output: MW_i, z_i, ρ_i

FIGURE 6

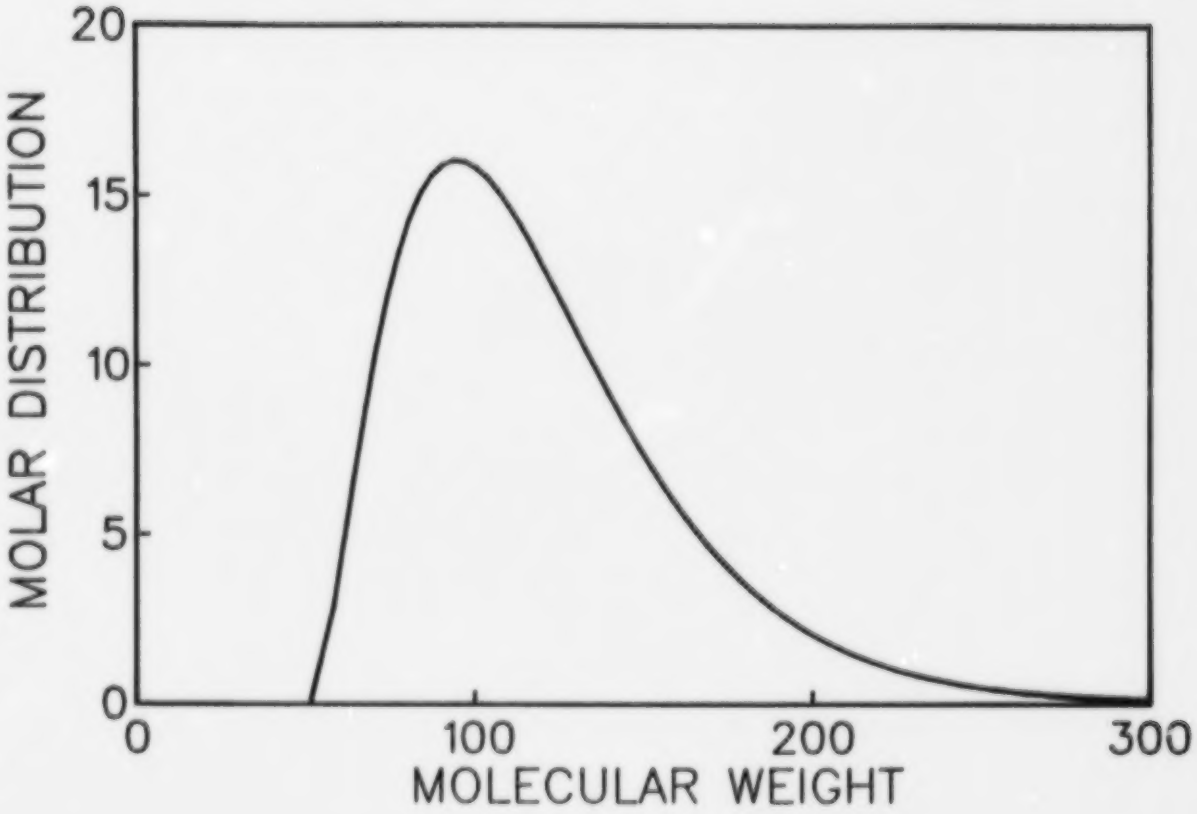

Feed composition of the 24 components
n-paraffin mixture

FIGURE 7

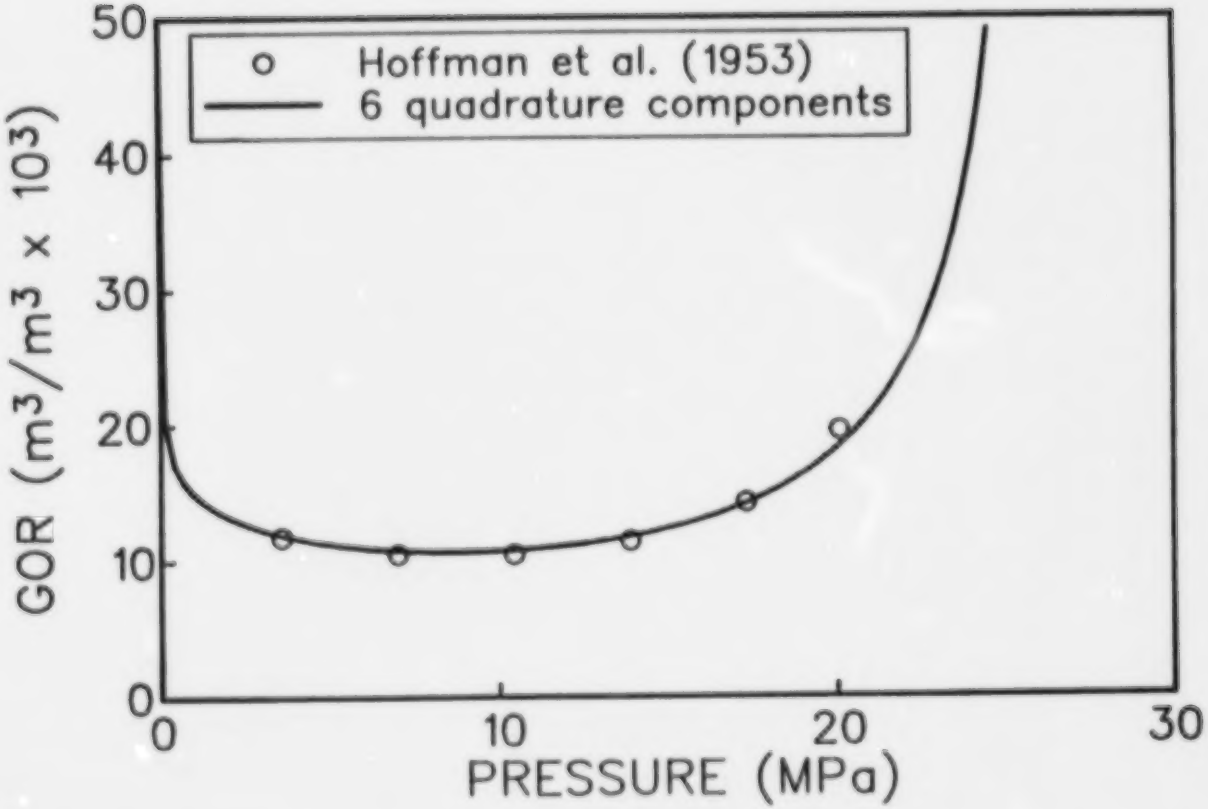

Gas–oil ratios for a natural gas mixture at 93.89°C

FIGURE 8

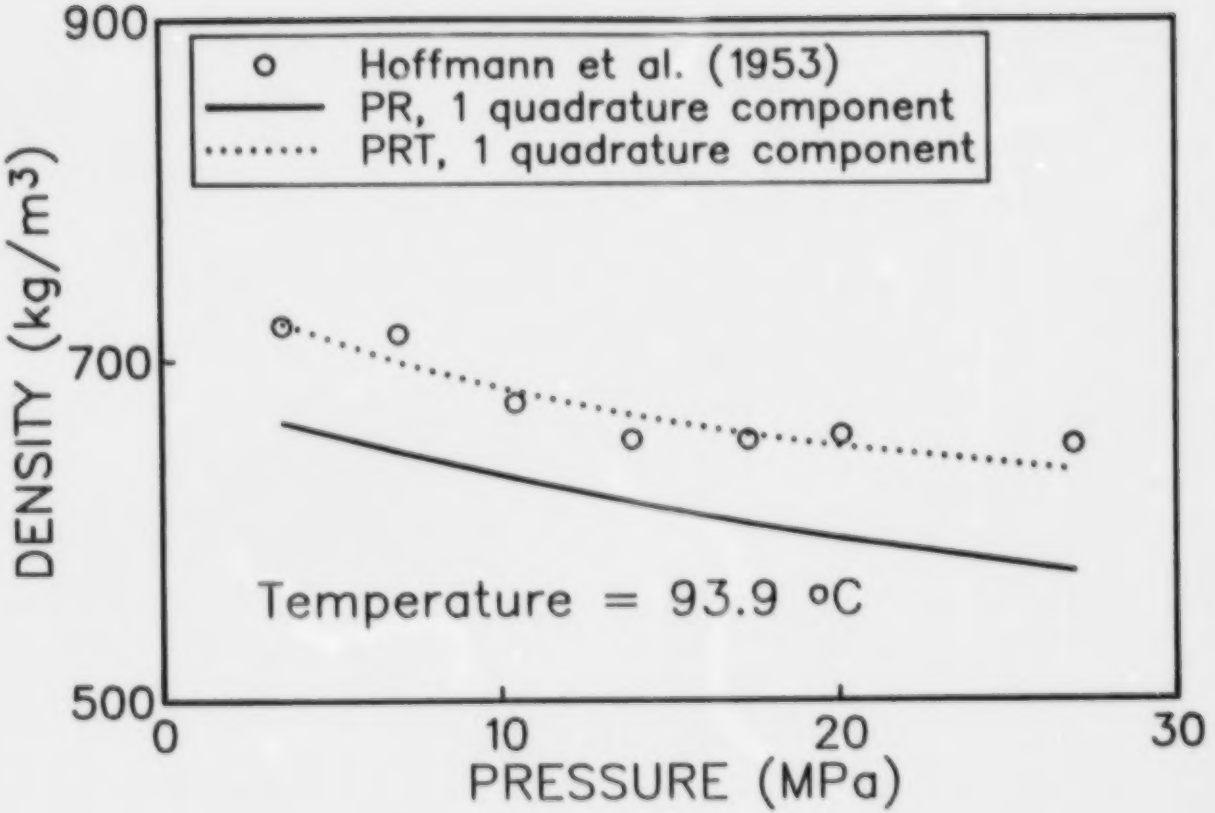

Comparison of density predictions for a gas–condensate system

FIGURE 9

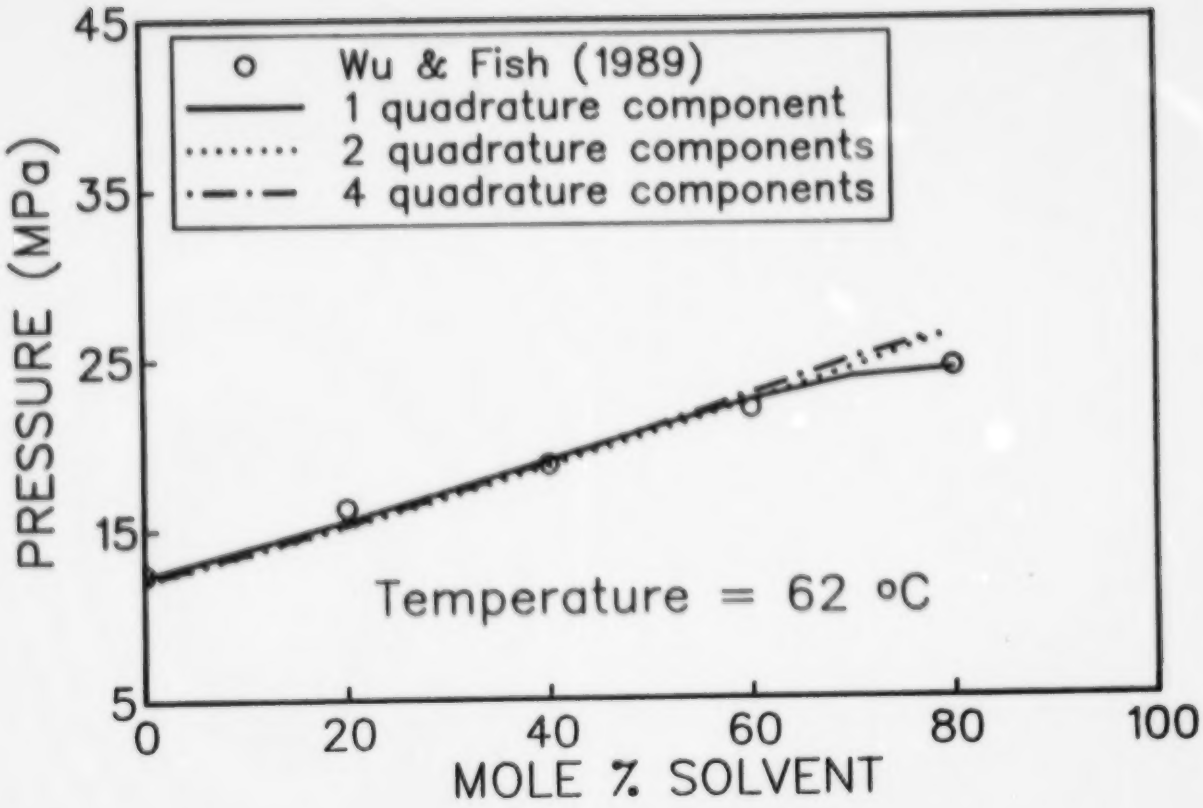

Saturation pressures for HC solvent/Oil 2 system

FIGURE 10

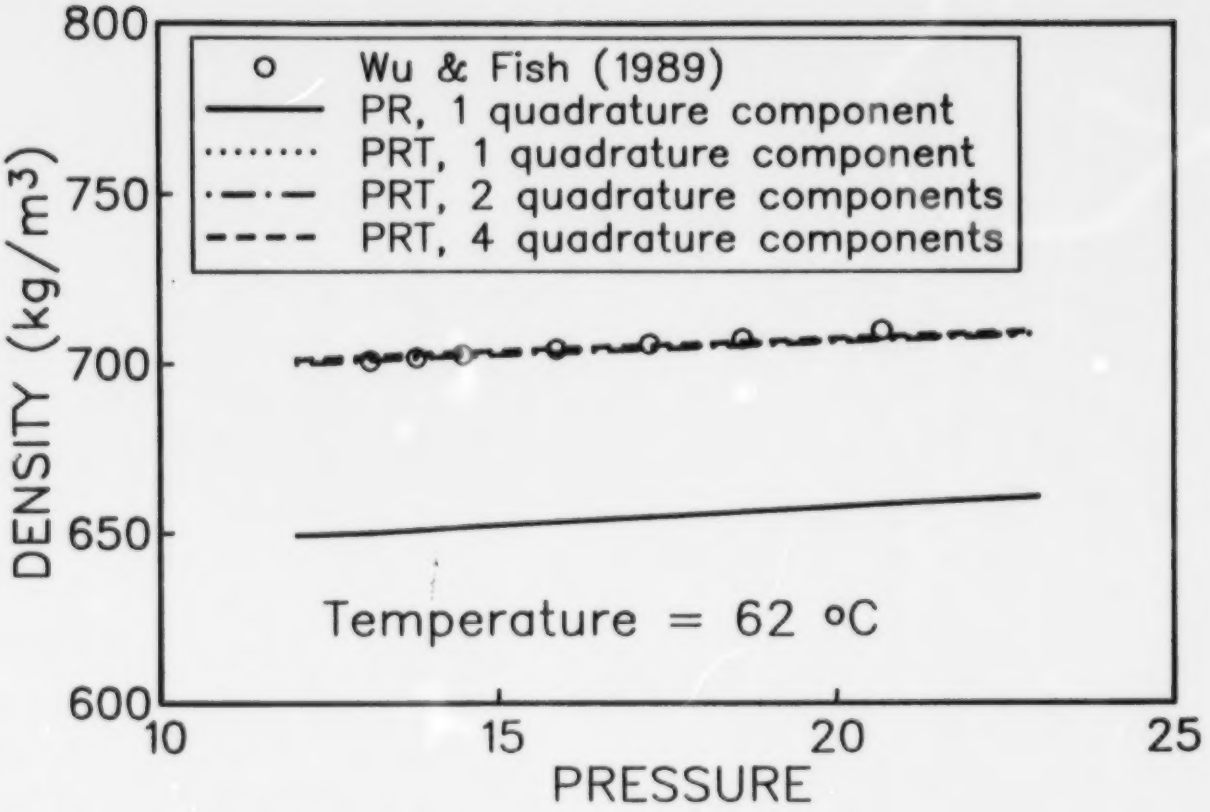

Comparison of saturated liquid densities of oil 2

FIGURE 11

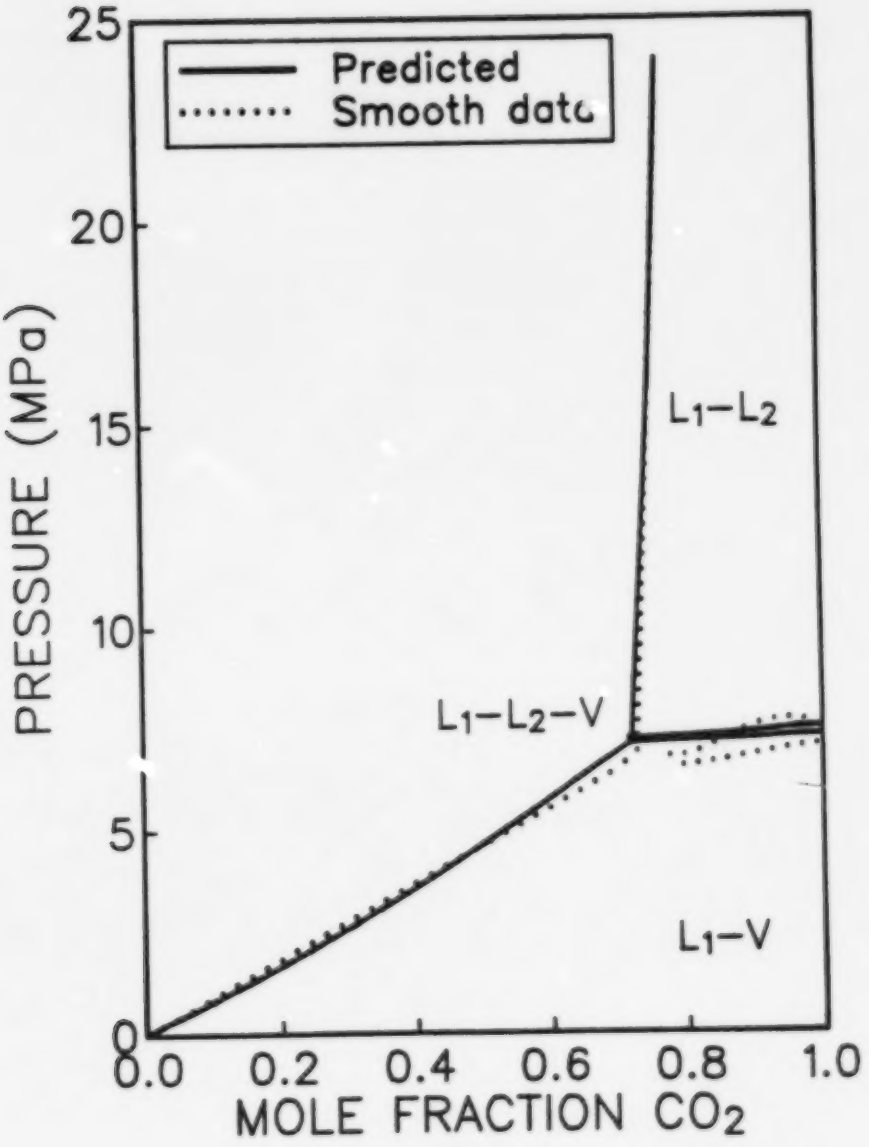

Phase behavior of mixtures of CO_2 with Maljamar separator oil at 32.2 °C

FIGURE 12

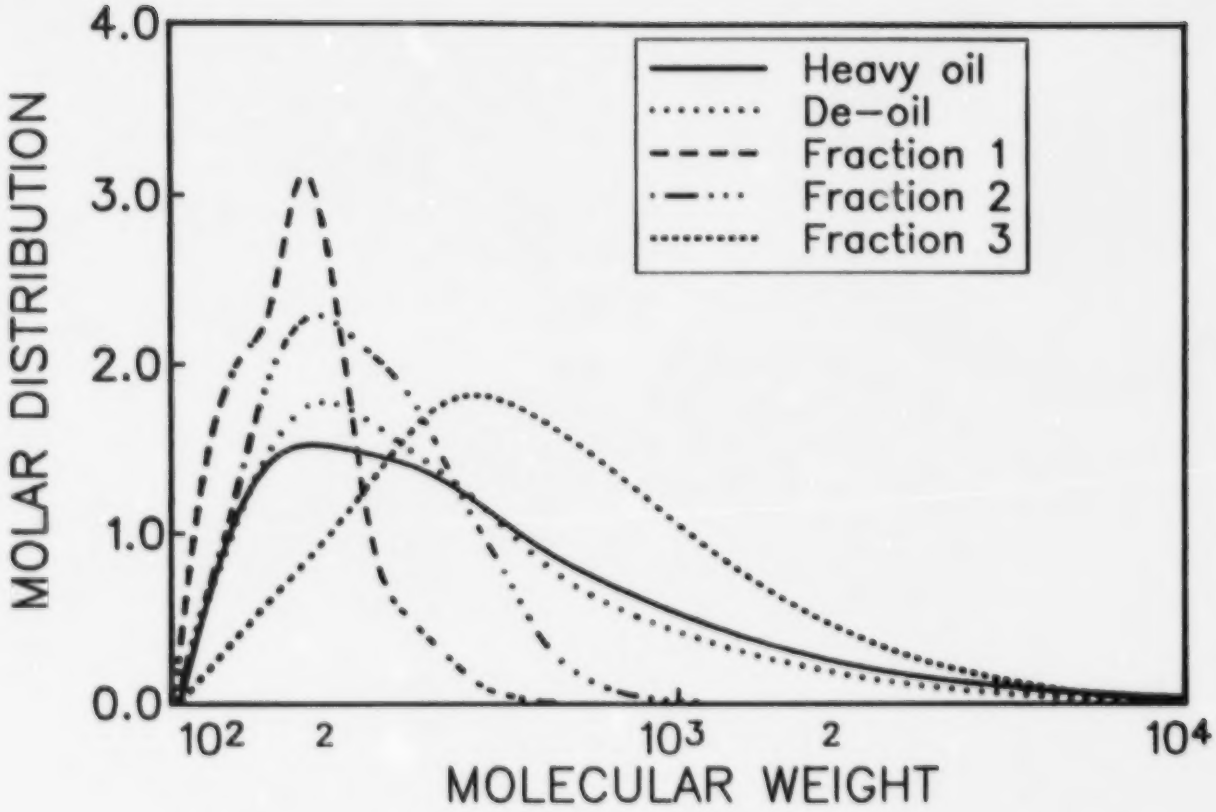

Molar distribution of Lindbergh heavy oil and its fractions

FIGURE 13

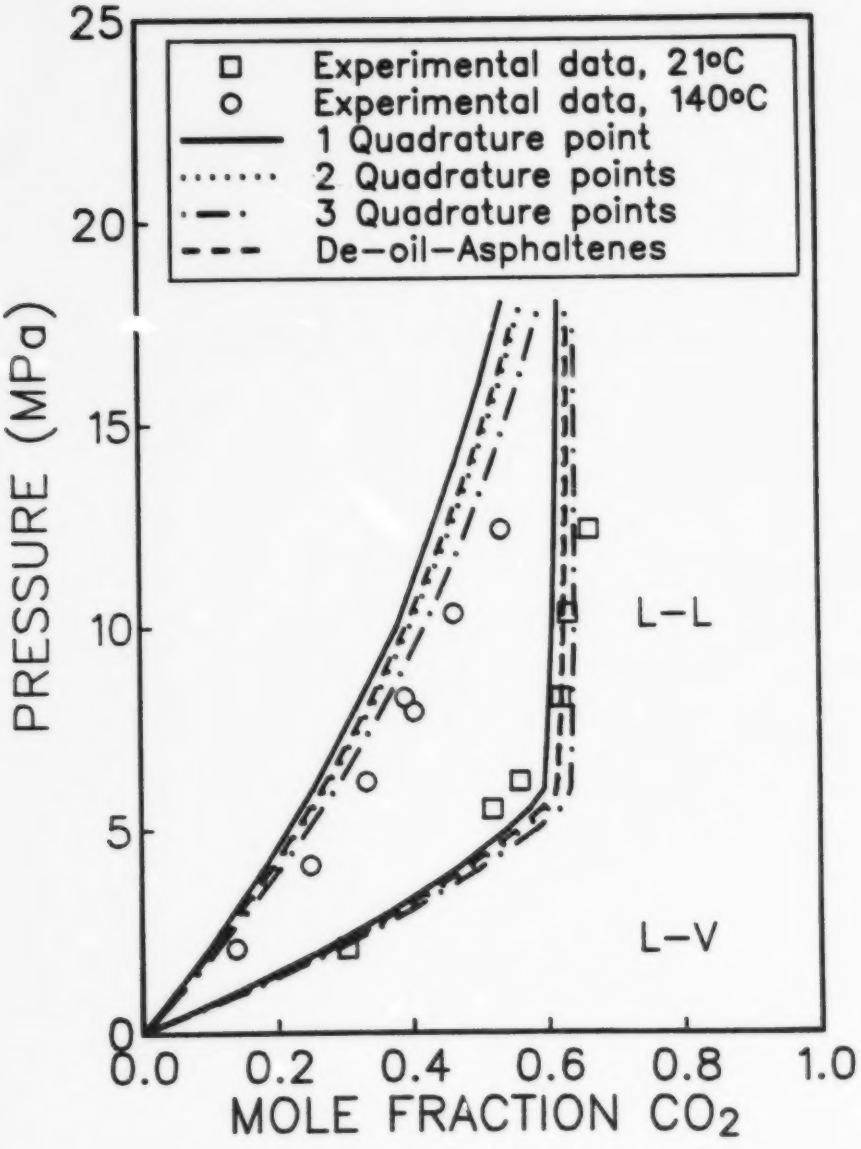

Phase behavior of Lindbergh heavy oil/CO_2 mixtures

FIGURE 14

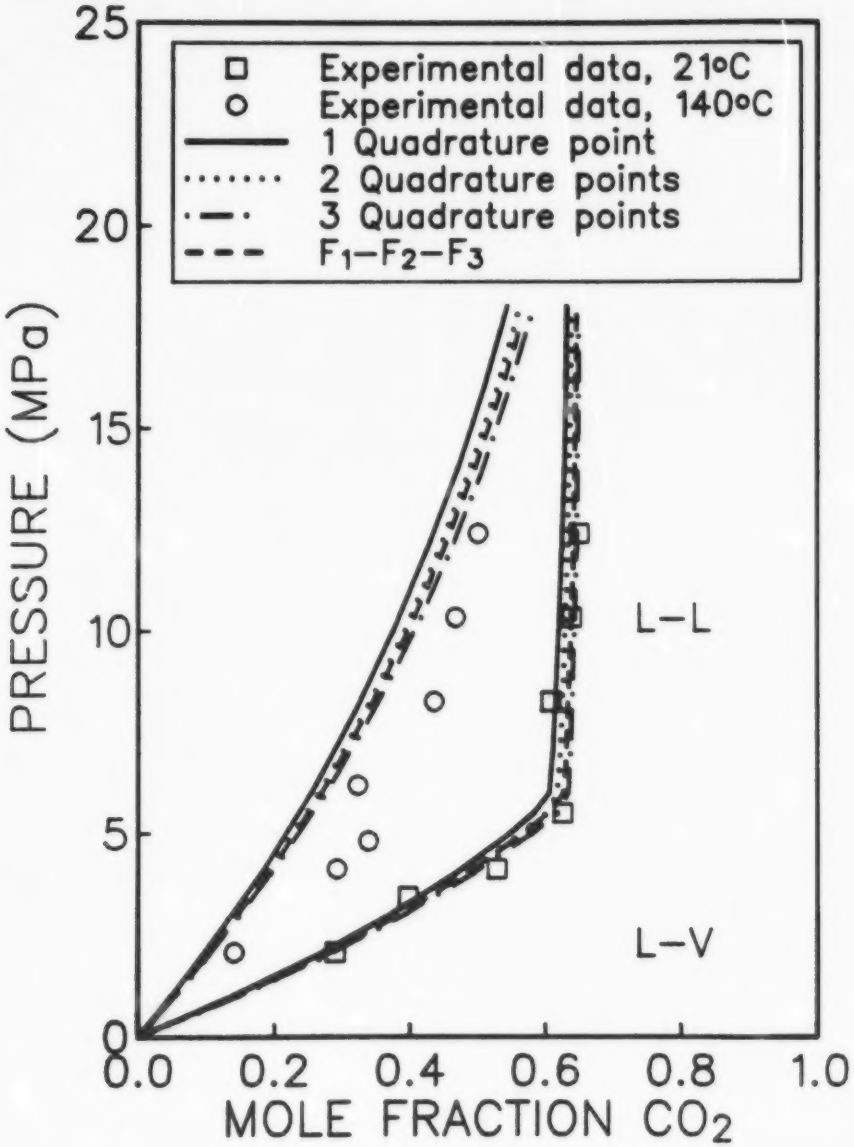

Phase behavior of Lindbergh De–asphalted oil/CO_2 mixtures

FIGURE 15

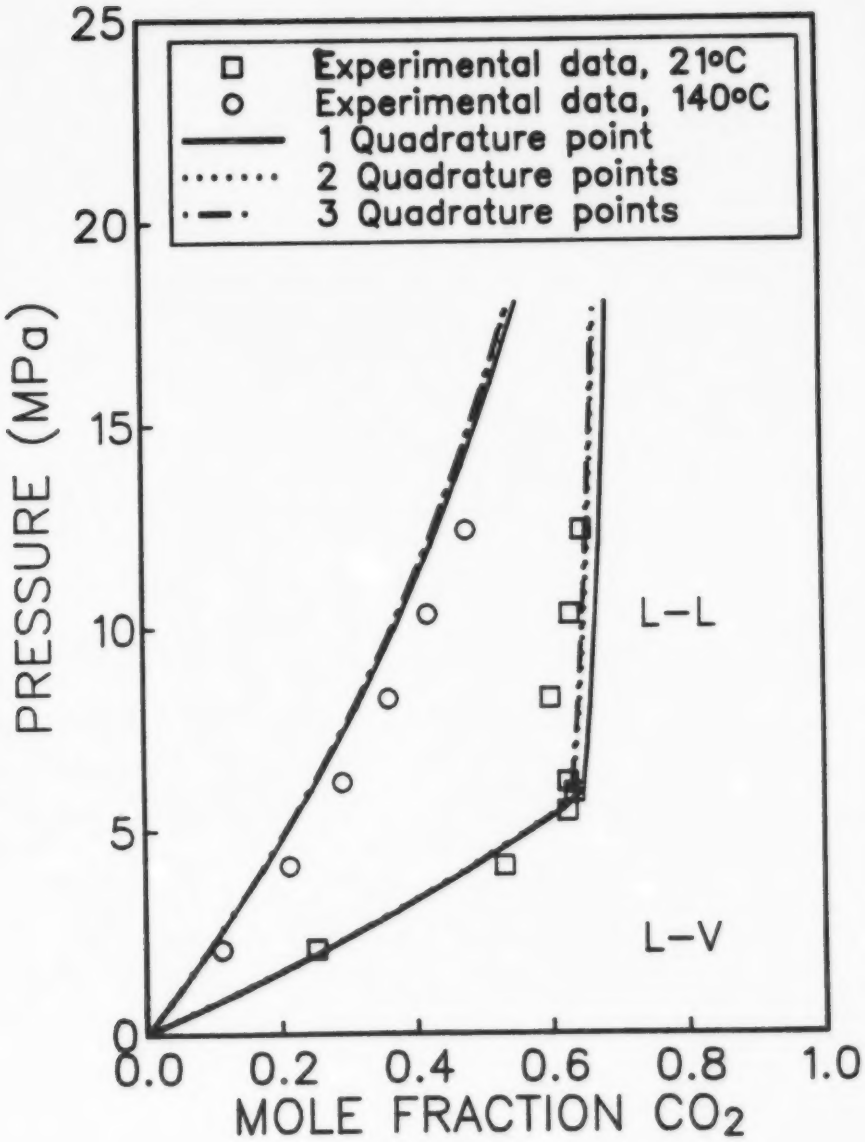

Phase behavior of Lindbergh Fraction 2/CO_2 mixtures

FIGURE 16

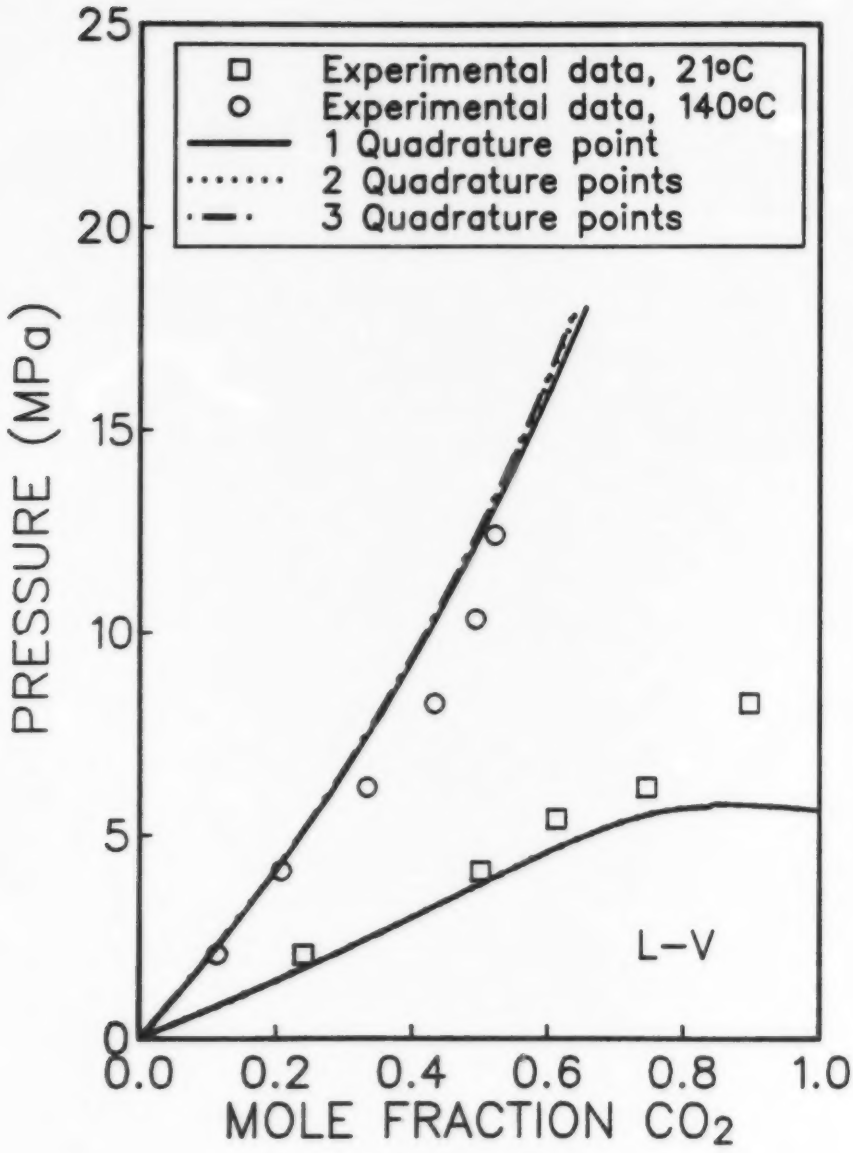

Phase behavior of Lindbergh Fraction 1/CO_2 mixtures

FIGURE 17

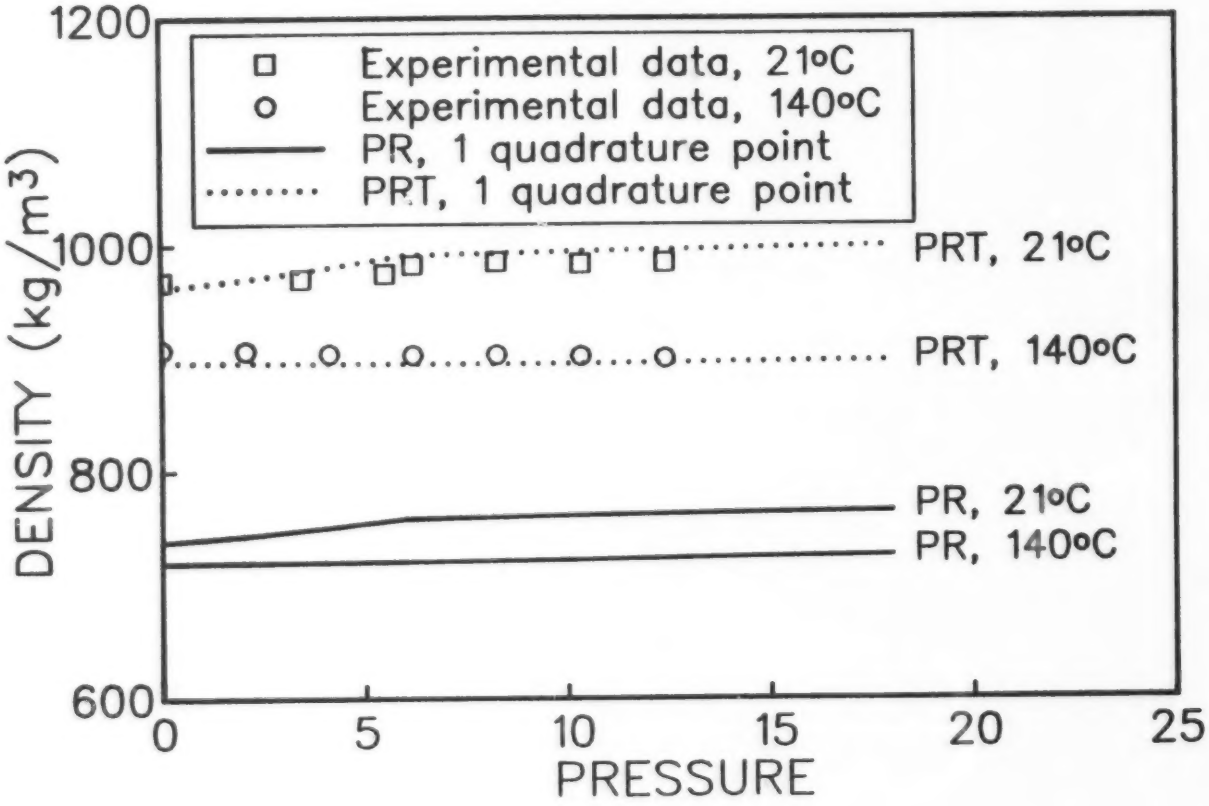

Density of Lindbergh heavy oil/CO_2 mixtures

FIGURE 18

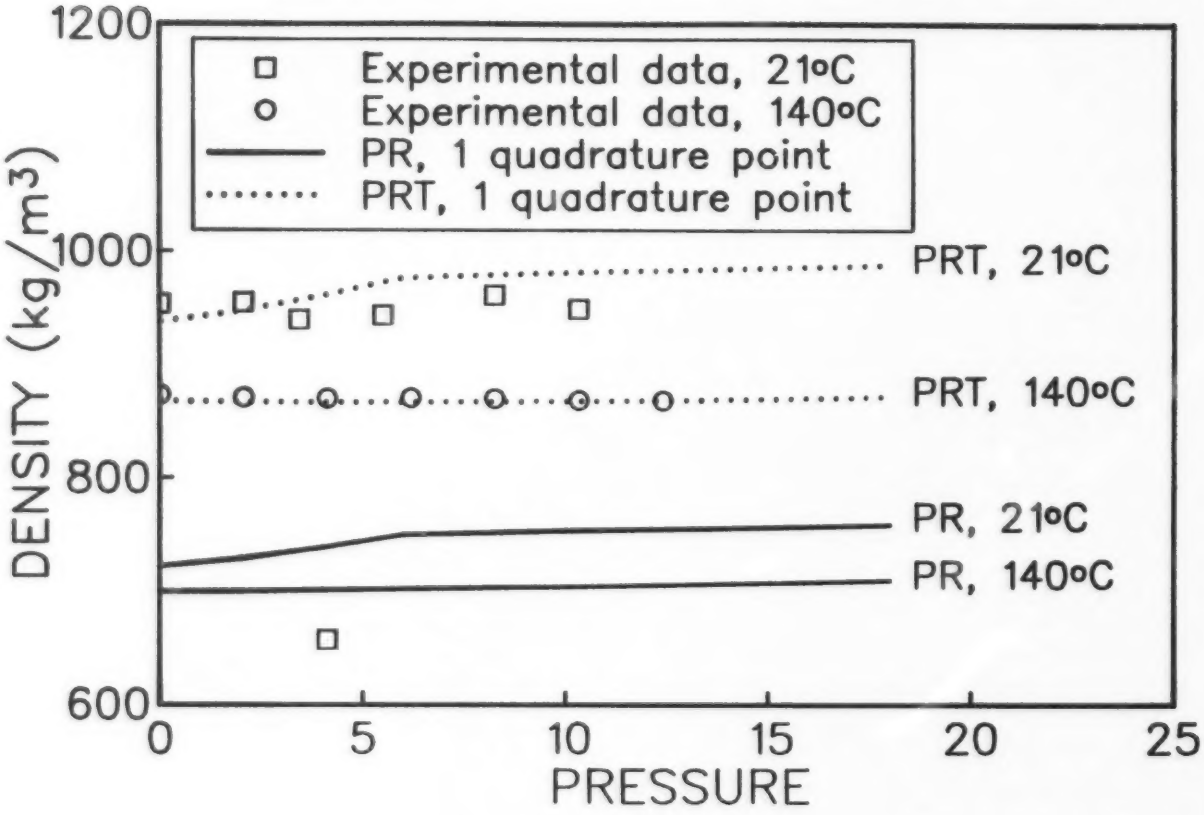

Density of Lindbergh
De-asphalted oil/CO_2 mixtures

FIGURE 19

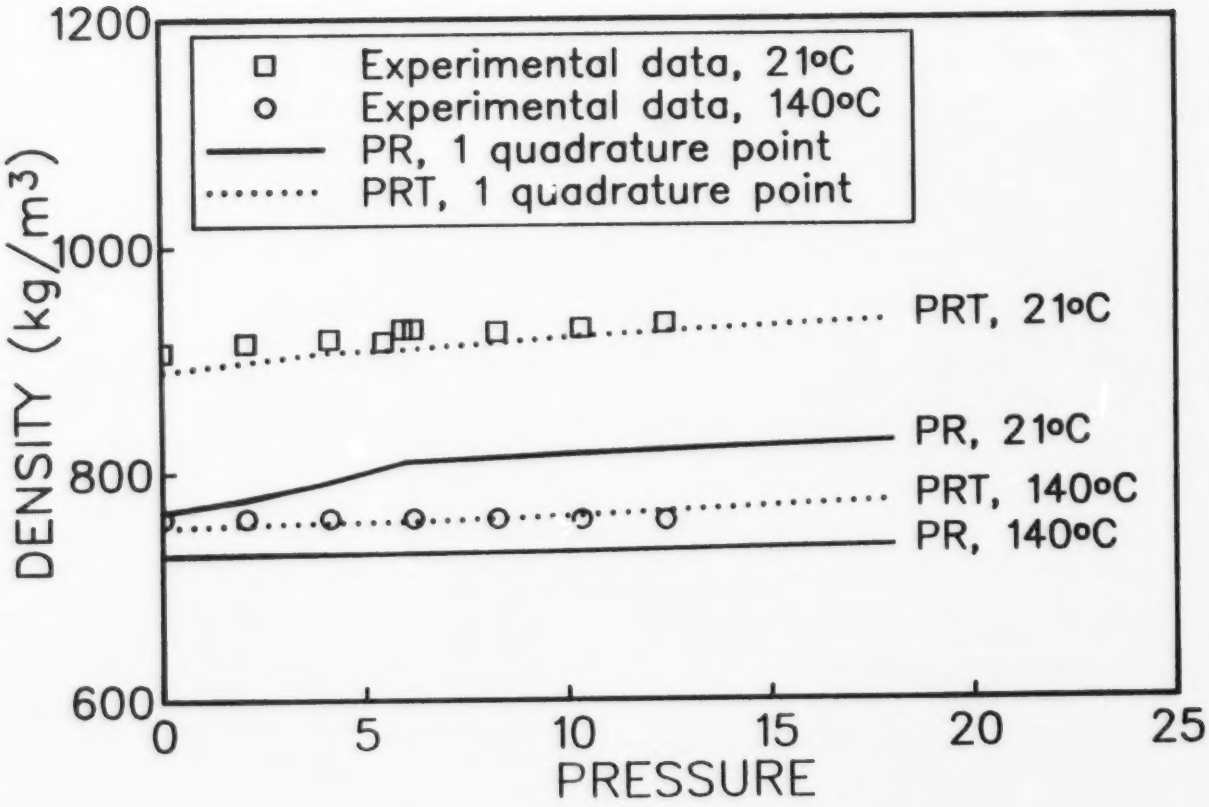

Density of Lindbergh
Fraction 2/CO_2 mixtures

FIGURE 20

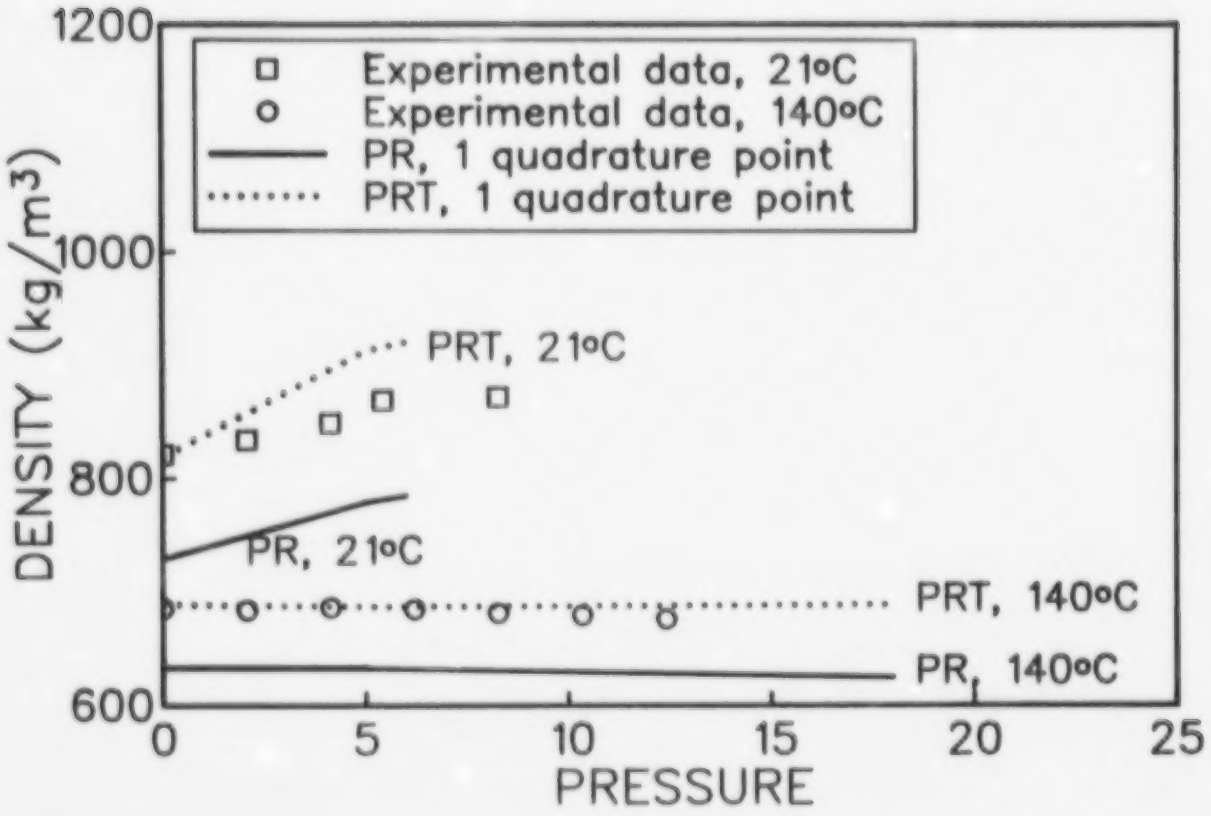

Density of Lindbergh Fraction 1/CO_2 mixtures

FIGURE 21

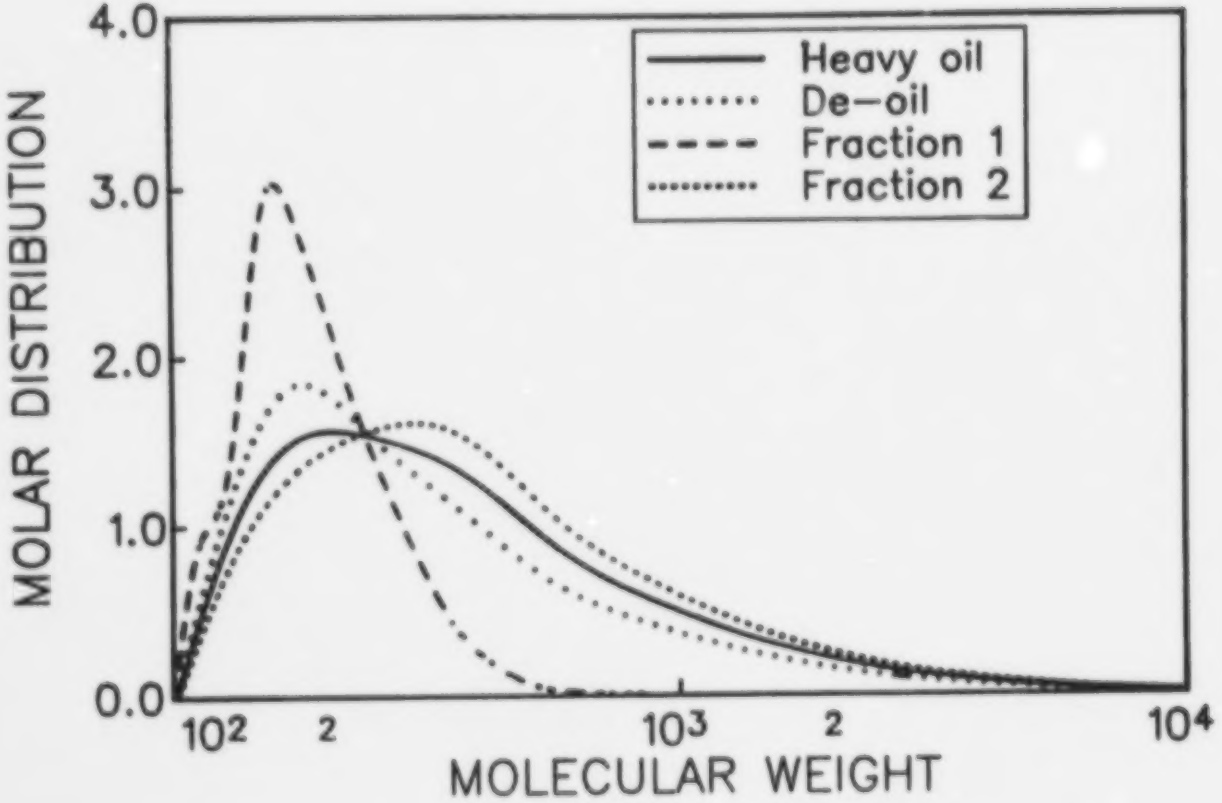

Molar distribution of Lone Rock heavy oil and its fractions

FIGURE 22

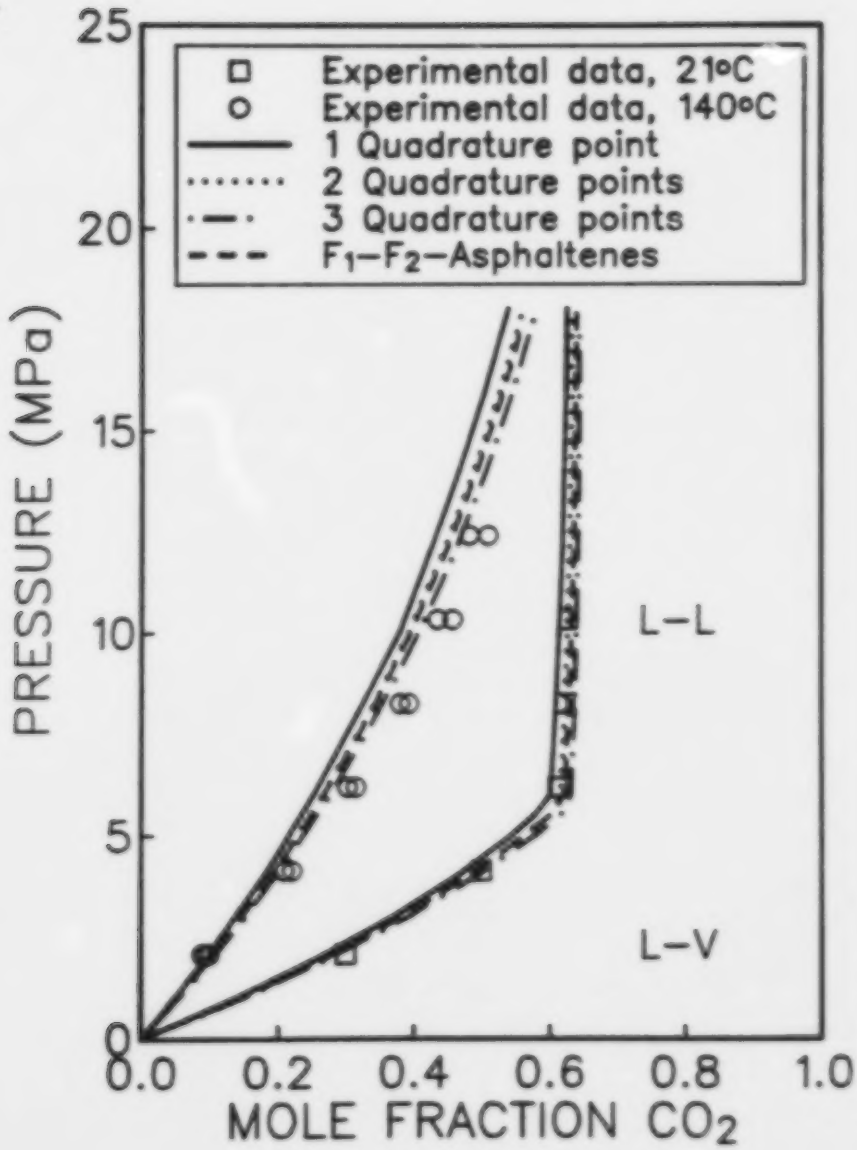

Phase behavior of Lonerock heavy oil/CO_2 mixtures

FIGURE 23

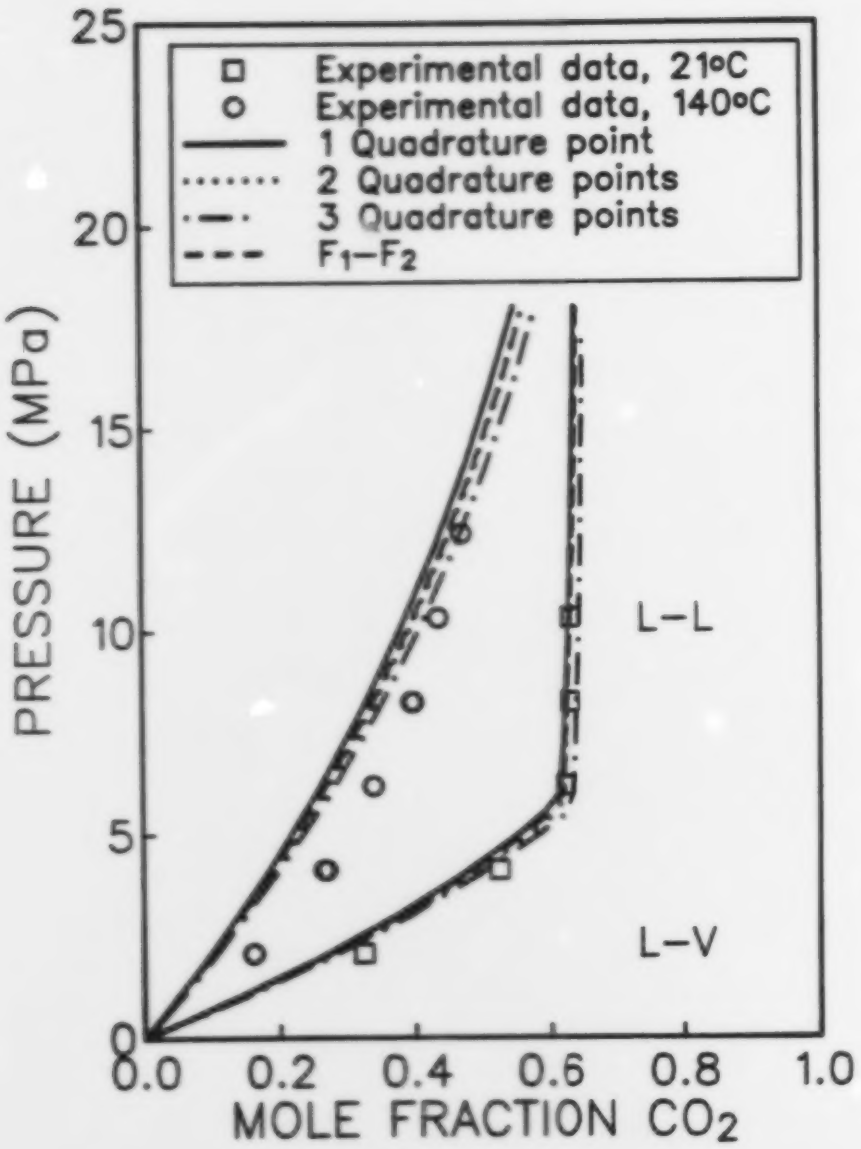

Phase behavior of Lonerock De-asphalted oil/CO_2 mixtures

FIGURE 24

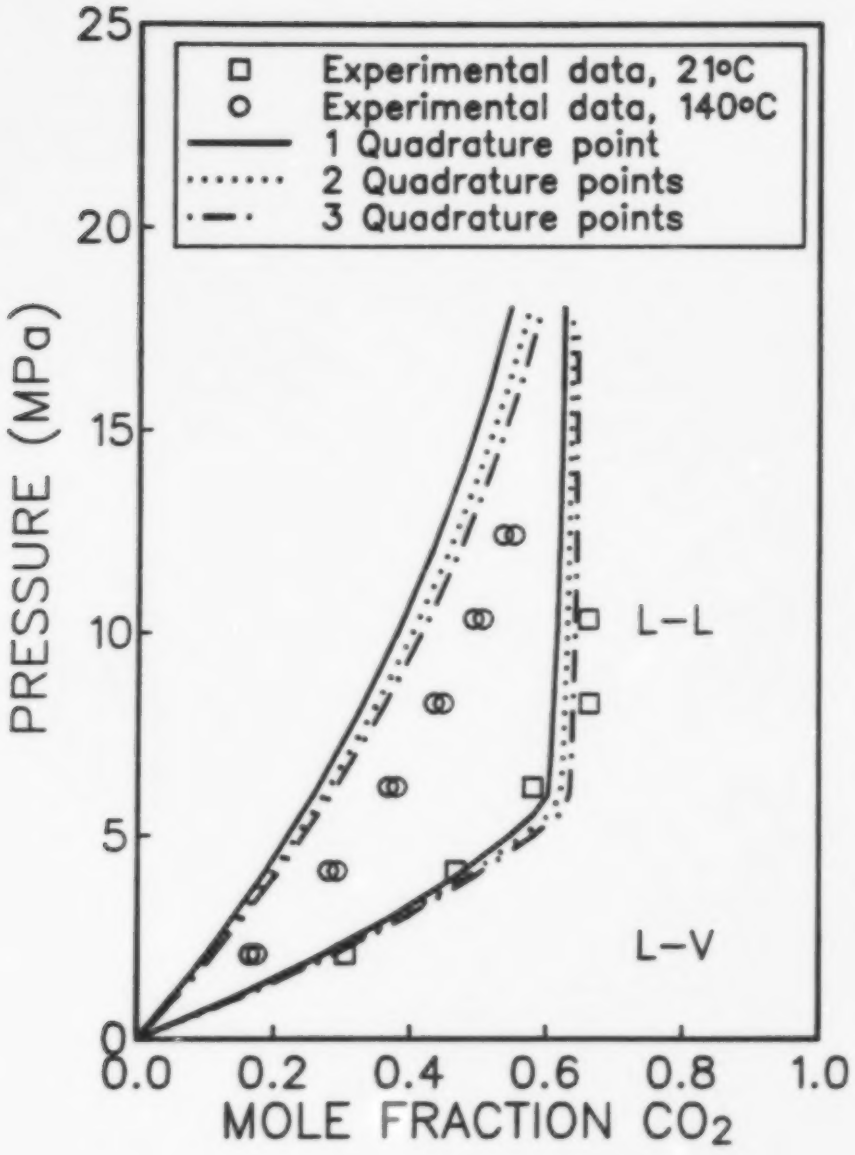

Phase behavior of Lonerock Fraction 2/CO_2 mixtures

FIGURE 25

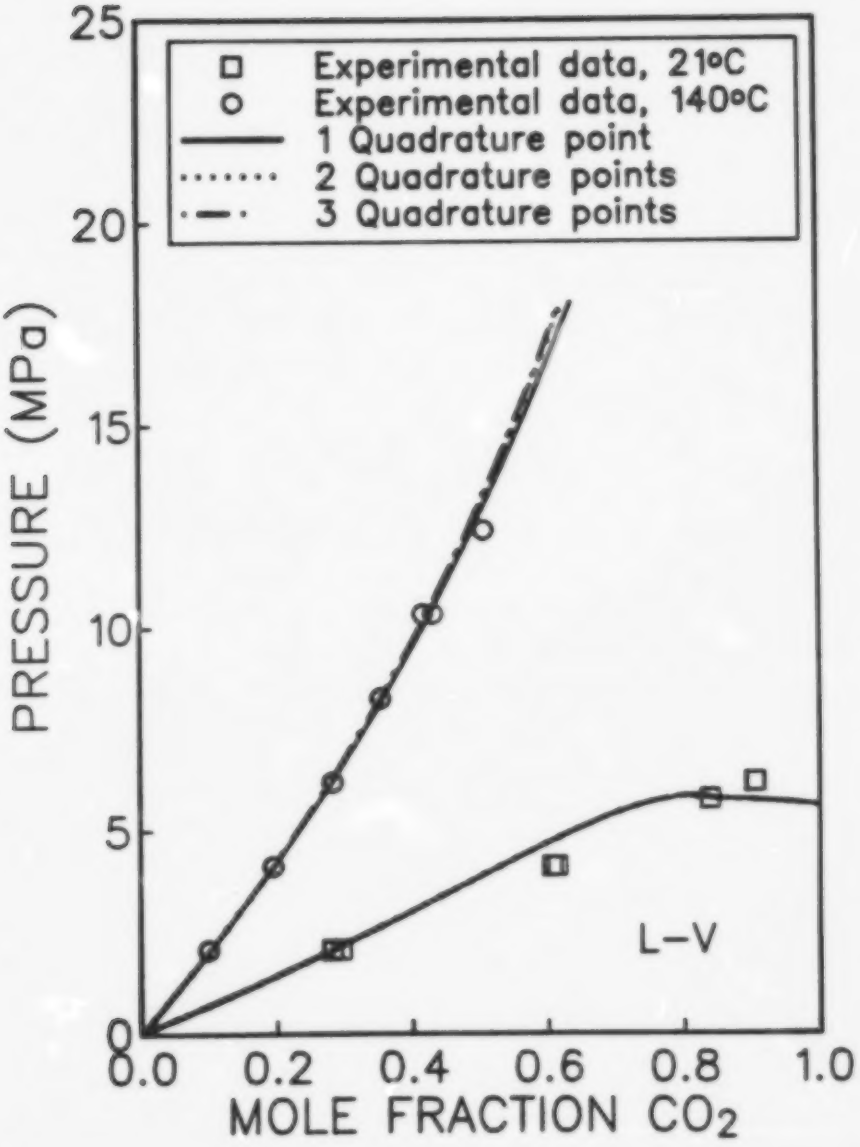

Phase behavior of Lonerock Fraction 1/CO_2 mixtures

FIGURE 26

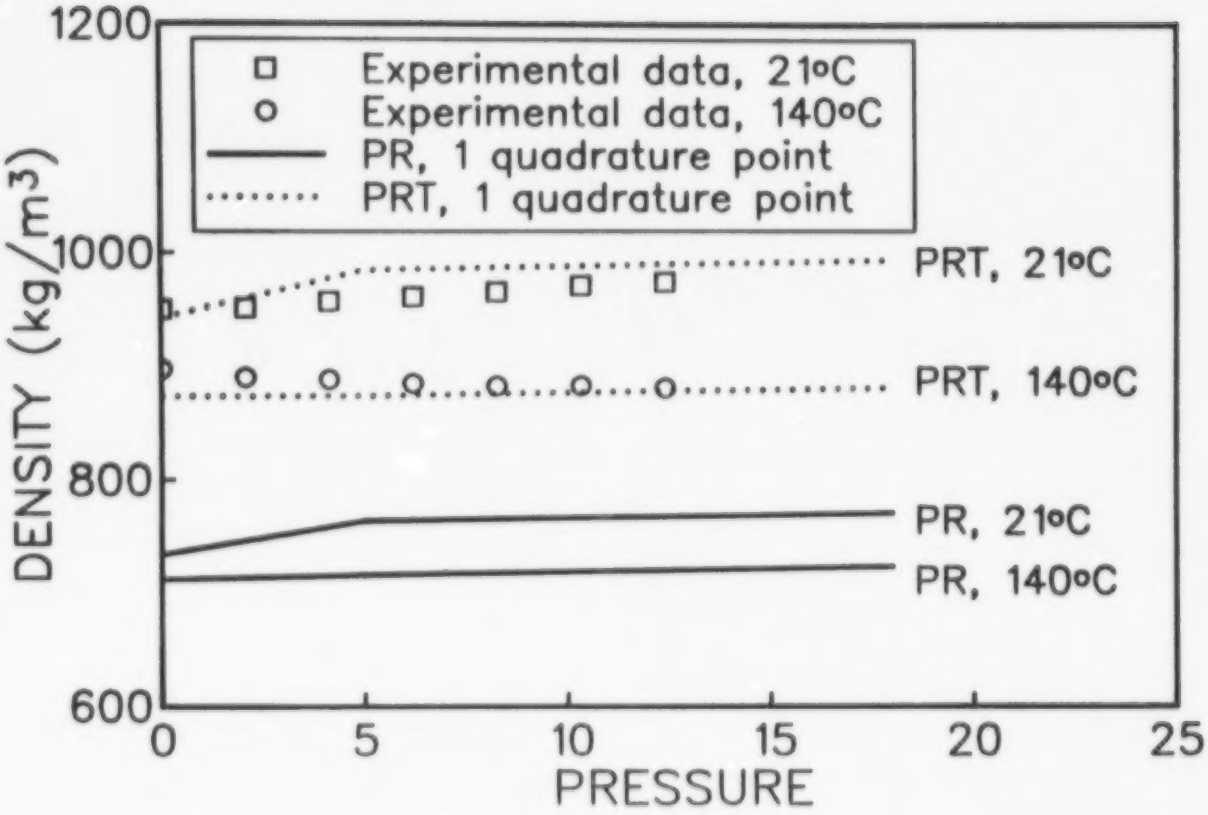

Density of Lonerock heavy oil/CO_2 mixtures

FIGURE 27

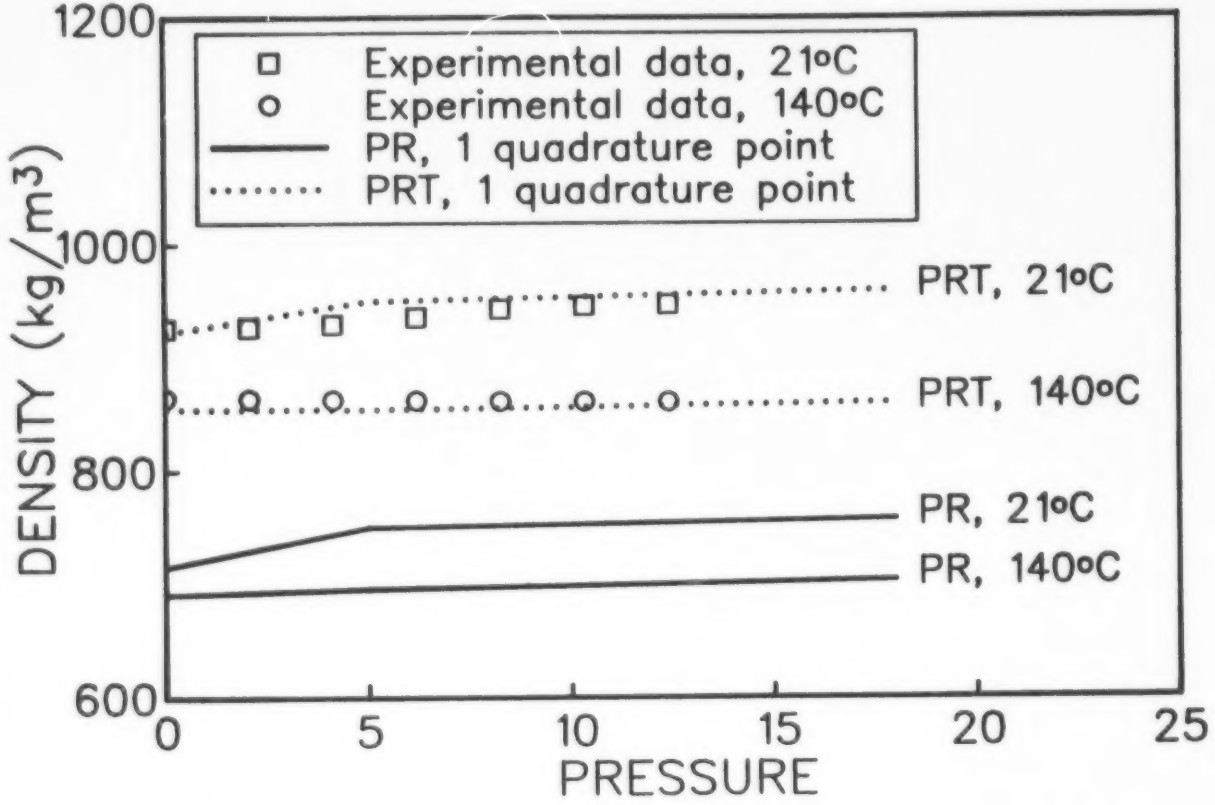

Density of Lonerock
De–asphalted oil/CO_2 mixtures

FIGURE 28

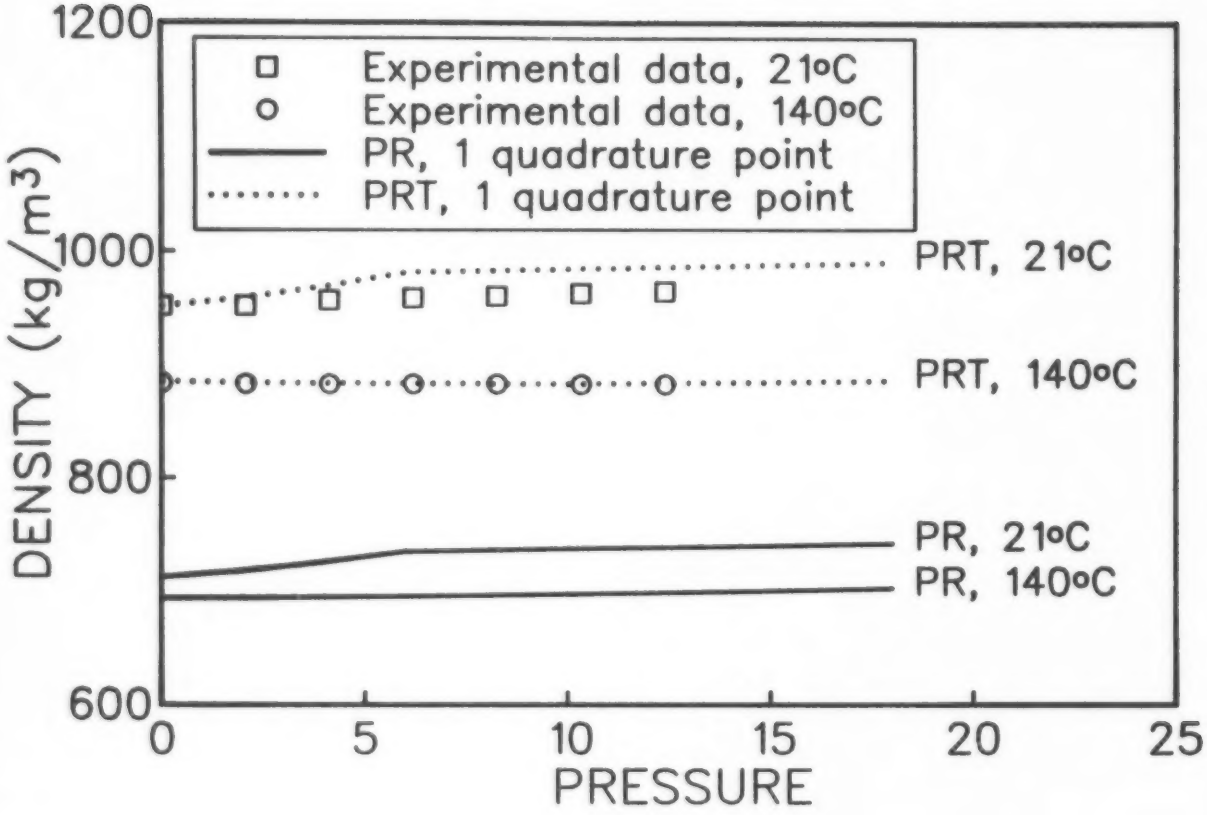

Density of Lonerock
Fraction 2/CO_2 mixtures

FIGURE 29

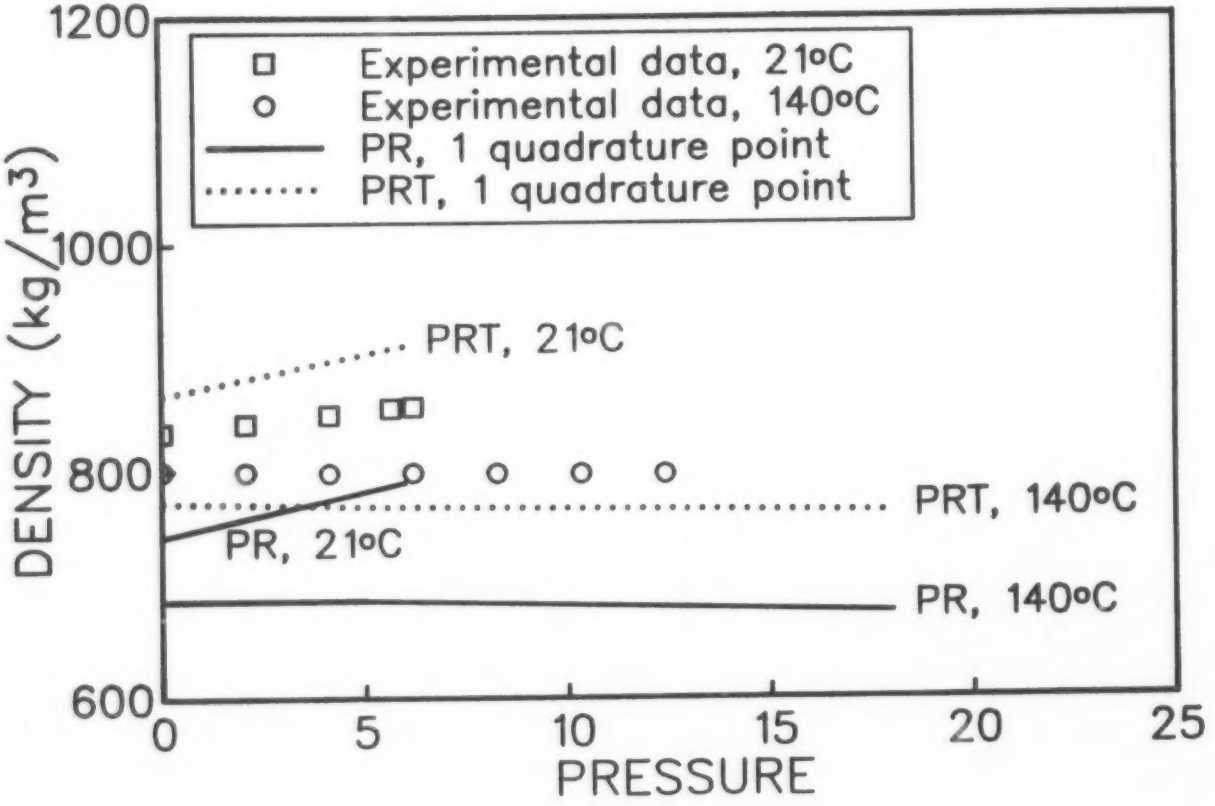

Density of Lonerock Fraction 1/CO_2 mixtures

FIGURE 30